UNIVERSIDADE DE LISBOA
FACULDADE DE CIÊNCIAS
DEPARTAMENTO DE FÍSICA

Comparison between Low-Cost and High-End sEMG Sensors for the Control of a Transradial Myoelectric Prosthesis

Alexandre Luís Airoso Calado

Mestrado Integrado em Engenharia Biomédica e Biofísica
Engenharia Clínica e Instrumentação Médica

Dissertação orientada por:
Alexandre Andrade
Giovanni Saggio

2017

ACKNOWLEDGEMENTS

This dissertation is dedicated to my loving parents. Thank you for making me believe in myself, without you, none of this would be possible.

I want to express my deep gratitude to Professor Alexandre Andrade, for all the orientation given throughout this dissertation, and to Professor Giovanni Saggio, not only for all the guidance, but also for the opportunity to work in such a stimulating research environment.

Thanks to Professor Luigi Bianchi for all the advice regarding classification.

I am also extremely thankful to Eng. Emanuele Gruppioni, not only for allowing my stay at INAIL to be possible, but also for all the help and availability. Also from INAIL, big thanks to Michele Fesani, whose help was very important during the second experiment.

Regarding the work elaborated in University of Rome "Tor Vergata", I must thank Antonio Pallotti and Mariachiara Ricci, who both helped me a lot, especially during the early stages of this work's development. Also, special thanks to Dr. Vito Errico, for all the help and for the kindness of reviewing this dissertation.

I also would like to thank the ERASMUS+ program, for granting me with a scholarship and providing support to develop my dissertation abroad.

Last, but not the least, thank you Elif, for all the love and support.

ABSTRACT

The loss of a hand due to amputation can completely change anyone's life. The autonomy to perform daily life tasks, which most of us take for granted, is drastically reduced, as well as one's quality of life. Fortunately, the use of a myoelectric prosthesis can help in overcoming such problems a transradial amputee must face every day. However, the current cost of such devices can limit its accessibility to economically less favored people.

In this dissertation, it is hypothesized that low-cost sensors can have a performance in controlling a myoelectric prosthesis as good as, or even better than the high-end sensors that are currently used in such applications. If this hypothesis can be validated, it may help in decreasing the costs of a myoelectric prosthesis and making it more accessible for the final user, the transradial amputee.

To compare both types of sensors, two experimental sessions were performed. The first one was performed only on able-bodied subjects and it had the objective of selecting the best combination of signal processing techniques and classifiers in order to use on the obtained sEMG signals.

In the second experiment, sEMG measurements were performed on both able-bodied and transradial amputated subjects. The signal processing techniques and classifiers that allowed to obtain the best results in the first experiment were used to classify the acquired data from all the subjects.

Overall, the accuracies calculated with the usage of the low-cost sensors, using some of the signal processing techniques, proved not to be significantly different from the ones obtained with the usage of the high-end sensors. This indicates that the usage of low-cost sensors in systems to control a myoelectrical prosthesis might indeed provide a performance as efficient as high-end sensor. Besides, it may provide the possibility to lower the overall cost of the currently available devices.

Keywords: sEMG sensors, classification, myoelectric prosthetics, transradial amputees, low-cost medical devices

RESUMO

A amputação é algo pode mudar completamente a vida de qualquer indivíduo. A autonomia para executar tarefas do quotidiano, que a maioria de nós toma como garantidas, é drasticamente diminuída. Para além da dificuldade acrescida neste tipo de tarefas, a autoconfiança do individuo também sofre um duro decréscimo, podendo até originar situações de depressão. Por todas estas razões, a qualidade de vida de um amputado transradial é severamente afetada de forma negativa. Felizmente, atualmente já existem vários tipos de soluções prostéticas para tentar lidar com todos os obstáculos consequentes de uma amputação. Entre estas, encontram-se as próteses mioelétricas. Este tipo de próteses pode recorrer ao uso de algoritmos de reconhecimento de padrões para associar certos padrões observados em sinais de sEMG provenientes do coto a diferentes gestos de mão, oferecendo a possibilidade ao amputado transradial de restaurar alguma da sua autonomia utilizando um dispositivo com funcionalidades semelhantes à mão humana. Porém, existem alguns obstáculos relacionados com a acessibilidade destes dispositivos, mais especificamente, o preço.

Atualmente, os preços das próteses mioelétricas comercialmente disponíveis são demasiados elevados, o que constitui um grande contratempo para indivíduos economicamente desfavorecidos que vivem com amputação transradial. Existe, portanto, a necessidade de diminuir os custos de produção e, consequentemente, o preço de mercado. No entanto, já existem alguns esforços a serem efetuados para tentar diminuir estes valores, tal como a impressão de algumas componentes em 3D. Para atingir este fim, também pode ser possível o uso de sensores de sEMG de baixo custo, ao invés de sensores sEMG de ponta. Porém, é necessário assegurar que a performance de controlo de uma prótese mioelétrica atingida pelo uso de sensores de baixo custo possa ser tão boa, ou superior à atingida pelo uso de sensores de ponta. Este é precisamente o grande foco desta dissertação.

Para efetuar esta comparação, recorreu-se ao uso do *Myo Armband* e sensores da marca *OttoBock*. O *Myo Armband* é uma bracelete comercial de baixo custo que permite o controlo de aplicações multimédia e contém oito sensores de sEMG. Por outro lado, os sensores da *OttoBock* são os elétrodos de eleição para aplicações prostéticas. Estes dois tipos de sensores foram aplicados em dois sistemas sEMG distintos e duas experiências foram efetuadas de modo a avaliar a performance de cada um.

Na primeira experiência foram efetuadas medições de sEMG nos antebraços de nove sujeitos saudáveis, com uso de ambos os sistemas. Foram usados diferentes algoritmos de reconhecimento de padrões para classificar segmentos do sinal sEMG correspondente a quatro gestos de mão diferentes. Em cada um dos sistemas foram usados cinco sensores.

A experiência foi dividida em duas sessões. O protocolo seguido em cada uma das sessões foi exatamente o mesmo e a aquisição de dados foi realizada de forma contínua. Foi pedido a cada um dos sujeitos para visualizarem um vídeo e replicar cada um dos gestos mostrados neste mesmo. Cada um dos quatro gestos selecionados foi repetido 10 vezes, durante 10 segundos. Este procedimento foi repetido para cada um dos sistemas em cada uma das sessões. Embora cada gesto tenha sido registrado durante 10 segundos, apenas os últimos 6 segundos foram usados para classificação. Isto foi feito com o intuito de usar apenas o sinal de sEMG estável e não o transiente, que é originado pelo movimento do sujeito entre diferentes gestos.

Diferentes técnicas de processamento de sinal e de extração de *features* foram aplicadas aos sinais adquiridos. Os dados obtidos, por sua vez, foram classificados por seis algoritmos diferentes,

incluindo *Linear Discriminant Analysis, Naïve Bayes, k Nearest Neighbours* e três variações de *Support Vector Machines.* Esta experiência teve, portanto, o propósito de avaliar quais poderiam ser as combinações mais favoráveis entre diferentes técnicas de processamento de sinal e classificadores, de forma a obter a máxima precisão de classificação possível.

Para avaliar as precisões calculadas, foram utilizados dois métodos de avaliação: *10-fold cross-validation* e treino-teste. Os testes estatísticos efetuados aos resultados adquiridos demonstraram a inexistência de quaisquer diferenças significativas entre ambos os sistemas, o que valida a hipótese principal proposta por esta dissertação. No entanto, é necessário validar esta mesma hipótese com dados extraídos de amputados transradiais, os utilizadores finais deste tipo de sistemas.

Na segunda experiência, as medições de sEMG foram efetuadas a doze amputados transradiais e a doze sujeitos saudáveis. Nesta experiência, em semelhança à primeira, também se realizaram duas sessões com protocolo igual. Contundo, comparativamente à experiência anterior, o protocolo usado sofreu algumas alterações. O número de sensores usados em cada um dos sistemas foi incrementado para oito e o número de gestos de mão foi aumentado para cinco. Os dados foram adquiridos de forma descontinua e a duração de cada aquisição realizada para cada gesto foi alterada para 2 segundos, de forma a obter apenas o sinal sEMG estável. Foram feitas 15 aquisições para cada um dos cinco gestos de mão, o que perfaz um total de 75 aquisições.

As combinações de técnicas de processamento de sinal e classificadores usados nesta experiência foram selecionados de acordo com os resultados da primeira. No total, foram usadas quatro diferentes combinações de técnicas de processamento de sinal, retiradas das seis usadas na experiência anterior, e dois classificadores, uma das variações da *Support Vector Machine* e *k Nearest Neighbours*.

As precisões calculadas voltaram a ser avaliadas novamente por meio de *10-fold cross-validation* e de avaliação treino-teste. Os resultados obtidos demonstraram a inexistência de diferenças significativas entre as precisões adquiridas para cada um dos sistemas, exceto segundo os resultados da *cross-validation*. Neste caso, o sistema da OttoBock permitiu o cálculo de precisões superiores às obtidas pelo sistema da *Myo Armband.* Contundo, as precisões deste último demonstraram ser bastante competitivas.

Nos resultados adquiridos, verificaram-se valores de precisão mais elevados no caso dos sujeitos saudáveis, em ambos os sistemas. Isto seria algo previsível, já que a não utilização diária do membro fantasma (a sensação de que membro amputado está ainda presente) leva a que o amputado se "esqueça" de como efetuava certos gestos com a mão que foi amputada.

De um modo geral, pode-se afirmar que não se verificaram diferenças significativas entre os resultados obtidos em ambos os sistemas, o que valida a hipótese principal proposta por esta dissertação. De facto, os sensores de baixo custo usados permitiram resultados de classificação tão bons como os obtidos com o uso de sensores de ponta. Contudo, é de notar que isto é apenas possível com uso de algumas técnicas de processamento ao sinal aos dados obtidos pelos sensores da *Myo*, nomeadamente a aplicação de um envelope e de um filtro passa-baixo com uma frequência de corte de 1 Hz. Sem qualquer tipo de processamento, os resultados obtidos com estes sensores foram bastante fracos. Por outro lado, os sensores da OttoBock, mesmo sem qualquer tipo de processamento de sinal, permitiram resultados bastante elevados, o que se deve ao facto de produzirem um sinal previamente filtrado, com envelope e amplificado, ou seja, um sinal de alta qualidade.

Considerando os resultados obtidos, é de facto possível que a aplicação de sensores de baixo custo a um sistema de controlo de uma prótese mioelétrica possa permitir uma performance tão boa

como a oferecida por sensores de ponta. Contudo, isto é apenas possível se o processamento de sinal usado for apropriado, assim como o classificador escolhido.

Em suma, é possível a substituição dos sensores atualmente usados em aplicações prostéticas por sensores com um custo mais reduzido, de modo a obter dispositivos mais económicos sem comprometer a qualidade do seu funcionamento. No entanto, antes destes sensores serem aplicados numa prótese mioelétrica, é necessário testar o sistema em tempo real e desenhar uma estratégia de controlo robusta, que permita uma boa comunicação entre as intenções do utilizador e as funcionalidades inerentes da prótese.

Palavras-chave: sensores sEMG, classificação, próteses mioelétricas, amputados transradiais, dispositivos médicos de baixo custo

CONTENTS

LIST OF FIGURES

LIST OF TABLES

ACRONYMS

ADC Analog-to-Digital Converter

EMG Electromyography

FFT Fast Fourier Transform

INAIL *Istituto Nazionale Assicurazione Infortuni sul Lavoro*

kNN *k* Nearest Neighbours

MAV Mean Absolute Value

MSE Mean Square Error

PLP Phantom Limb Pain

QP Quadratic Programming

SD Standard Deviation

sEMG Surface Electromyography

SMO Sequential Minimal Optimization

SMU Single Motor Unit

SVM Support Vector Machine

LDA Linear Discriminant Analysis

1 INTRODUCTION

Amputation occurs when a body extremity must be removed. This can happen due to several reasons, traumatism being the most common, followed by neoplasia and infectious or vascular diseases [1]. According to K. Ziegler-Graham et al. [2], just in the United States, there are over 2 million people living with limb loss and approximately 185,000 amputations occur each year [3]. Just in 2005, around 541,000 Americans were submitted to an upper limb amputation and it is predicted that this number will double by 2050 [2]. On the other hand, there are 3500 and 5200 upper limb amputations that occur in Italy and in the U.K., respectively, each year, 12% of which are transradial [4]. Transradial amputation is the definition given for when the radius and ulna are sectioned and the lower portion of these bones, along with the hand, are removed from the body.

Amputation is often followed by the sensation that the removed body extremity is still present. "Phantom limb" is the term used to describe the no longer existing part of the body felt by the amputee. These sensations include the feeling of a specific position, shape or movement of the missing limb [5]. 50-80% of all amputees suffer from a condition called "Phantom Limb Pain" (PLP) [6], which is described by pain in the body part that is no longer present, that is, the phantom limb. The level of pain caused by PLP can vary according to different physical and psychological factors and its quality is described in different ways, such as stabbing, throbbing, burning or cramping [5].

The loss of a hand, obviously decreases one's quality of life, affecting the autonomy to perform simple daily tasks. Fortunately, nowadays there are several prosthetic solutions available to try to overcome these problems by replacing the functions and appearance of the amputated limb. The upper limb prostheses can be divided into two categories: passive, which comprises cosmetic and functional, and active, which comprises body-powered and externally powered. The cosmetic prostheses have the only function of having an aesthetic appearance and to try to simulate, as much as possible, the appearance of a real limb, which is useful to improve the amputee's confidence and social interaction. The functional ones have a more specific purpose, which aims to facilitate tasks related with a specific type of work or sport. On the other hand, body-powered prostheses use cables to link the movement of the body to the prosthesis and subsequently control it. If the user moves the body in a certain way, the cables attached will cause the opening or closing of the prosthesis, for example. However, it can quickly cause fatigue on the user, which is the main downside of this type of prostheses. Finally, the externally powered prostheses offer an external power supply that can provide energy for the execution of the desired movements without too much effort from the user. They can be divided into myoelectric, which are controlled by EMG (electromyographic) signals, and electric, which can be controlled by the use buttons [4].

Myoelectrical prostheses rely on Surface Electromyography (sEMG) signals from the remaining muscles present in the residual limb (or stump). The myoelectrical prosthesis interprets the muscle signals voluntary generated by the user to control the actuators, which in the case of a transradial amputee can be a robotic hand. However, only a quarter of patients with upper limb amputation use this kind of prostheses [7]. The main problem lies on the concentrated effort to acquire a higher movement accuracy while ignoring the need for a robust control system, making its application on daily living harder than it should [8]. The biggest challenge when designing a control system for a myoelectrical prosthesis is to make sure there is a good trade-off between the user's intentions and the inherent capabilities of the prosthesis, therefore the focus should lie on creating an intuitive control system

without sacrificing robustness because, in this kind of medical equipment, a bad decision is more dangerous and has a bigger impact on performance and usability than abstention [9].

Another big issue is the high price of myoelectric prostheses. According to the Bioengineering Institute Center for Neuroprosthetics, at the Worcester Polytechnic Institute [10], the price of a myoelectric prosthesis with a functional, realistic-looking, hand can cost up to $20,000-$30,000 or more, depending on the level of upper limb amputation. Another study from the United States Department of Veterans Affairs states that a myoelectric prosthesis for partial loss of a hand costs $18,703 and up to the middle of the lower arm, $20,329 [11]. Furthermore, during the user's lifetime, the prosthesis will have to be replaced several times. For example, the estimated average lifetime cost of prosthesis medical care for a veteran of the Iraq or Afghanistan wars is $823,299 [11]. More advanced myoelectric prostheses, like the Michelangelo Hand from OttoBock [12], can cost around $100,000 [13]. Due to the high costs of acquiring and maintaining a prosthesis, it is essential to decrease the production and selling costs without compromising the quality and reliability of the prostheses, so that this kind of devices can be accessible to any person living with transradial amputation. This subject will be one of the focus of this work.

1.1 THE CONTEXT

The work described in this dissertation was elaborated over a course of an internship of approximately 6 months, from the 5th of February to the 15th of August of 2017, in the department of Electronical Engineering from University "Tor Vergata" in Rome. Three weeks from this internship were spent in the INAIL (*Istituto Nazionale Assicurazione Infortuni sul Lavoro*) prosthesis center, in Budrio (in the province of Bologna), from the 3rd to the 22nd of July, with the purpose of making EMG measurements on amputees.

The main objective of this dissertation is to compare low-cost sEMG sensors with high-end, state-of-the-art sEMG sensors and evaluate if their performances can be similar for the control of a myoelectric prosthesis or a virtual arm based on pattern recognition algorithms for the classification of different hand gestures, using different signal processing techniques. The selected devices for the task at hand were the Myo Armband [14] and sEMG sensors manufactured by OttoBock. The Myo Armband is a low-cost commercial device which is used on the forearm to control video-games, music and visual entertainment, and it has a cost of $199. On the other hand, the OttoBock sensors (model 13E200=50) [15] are the standard electrodes used for clinical prosthetic applications and each one has a price of around $400 (total cost for all the sensors is $3,200, without considering the elastic band and the data acquisition and transmission components, that are integrated in Myo Armband).

If it is proven that low-cost commercial sensors, such as the ones from Myo Armband can achieve results as good as, or even better than high-end sensors, such as the OttoBock sensors, then it could be possible to decrease the production costs of prostheses without compromising the device's performance and making it more accessible to the final user: the amputee.

1.2 STRUCTURE OF THE DISSERTATION

The present dissertation is constituted by six chapters, where chapter 1 is the present introduction.

In chapter 2, various theoretical concepts are thoroughly explained to integrate the reader within the context of this dissertation. It features a revision about forearm anatomy, a state-of-the art about Surface Electromyography and its use for a wide range of application and a review of pattern recognition algorithms.

Chapter 3 contains a description of the materials used throughout this dissertation, both *hardware* and *software*. The systems built with low-cost and high-end sensors are thoroughly described.

Chapter 4 describes the methods and discusses the result from experiment 1. This experiment was done to validate the main hypothesis of this work in able-bodied subjects, before performing measurements on transradial amputees. It was also helpful to select the signal processing methods and classifiers that allowed for best results while using sEMG signals.

Chapter 5 describes the methods and discusses the results from experiment 2. This experiment was performed on both able-bodied and transradial amputated subjects and it was performed to validate the main hypothesis in this dissertation on both subject groups.

Finally, in chapter 6 the main conclusions drawn from the overall results obtained in this dissertation are presented and discussed.

2 BACKGROUND

2.1 ANATOMY OF THE FOREARM

Since the focus of this work will fall on transradial amputees and on EMG signals generated by the forearm muscles, it is important to understand its anatomy. Due to the usage of surface EMG sensors, the most superficial muscles of the forearm are the ones that matter the most. The signals generated by these muscles will be the most visible and with most intensity.

In Figure 2.1, it is possible to observe the most superficial muscles of the forearm from an anterior view and in Figure 2.2 from a posterior view. The muscles responsible for hand, wrist and finger movements are called extrinsic hand muscles. Although these muscles are in the forearm, they have tendons that extend to the hand.

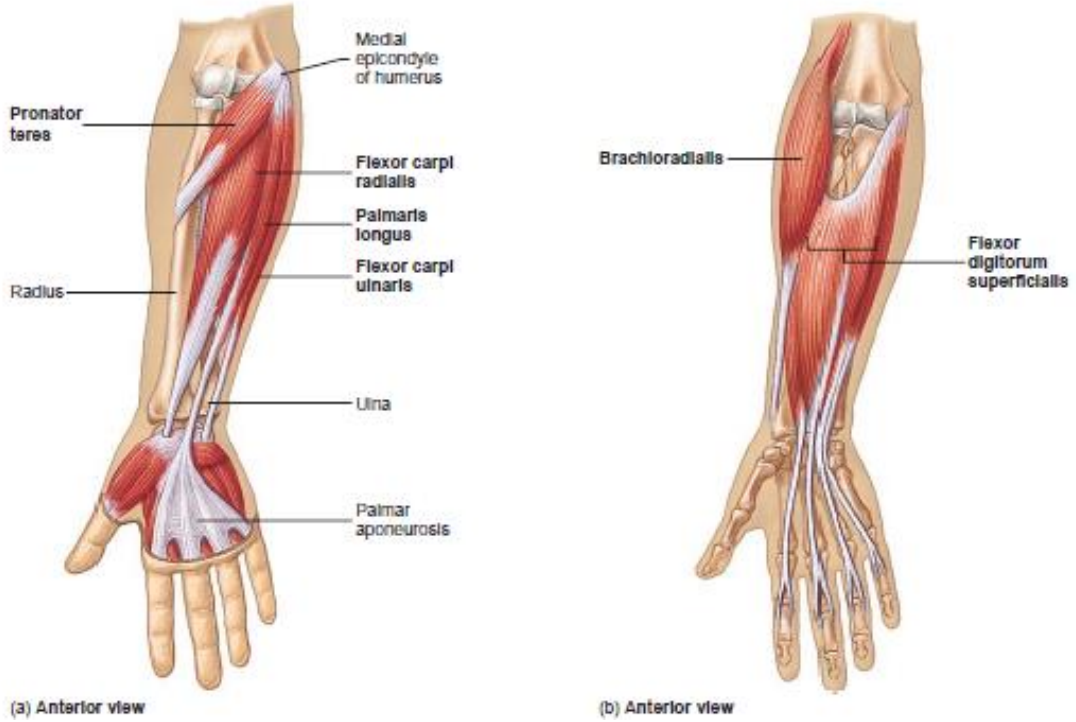

Figure 2.1: Anterior view of the right forearm superficial muscles (a) and with a deeper view (b) [16]

Considering only the superficial muscles, *Flexor carpi radialis* and *flexor carpi ulnaris*, the two most important anterior muscles, are responsible by the flexion of the wrist and the *extensor carpi radialis longus* and the *extensor carpi ulnaris* for the extension. The *palmaris longus* also aids in the flexion of the wrist and tenses palmar fascia. The *flexor digitorum superficialis* takes part on the flexion of the four medial digits while the *extensor digitorum* extends only the little finger, along with the wrist. Finally, the *brachioradialis* is the muscle responsible by the flexing of the forearm at the elbow but it is also responsible for pronation and supination.

For the context of this work, the anatomy knowledge of the forearm presented is sufficient because of the reasons stated above, if the interested reader wants to know more about this subject, please read chapter 10 of [16].

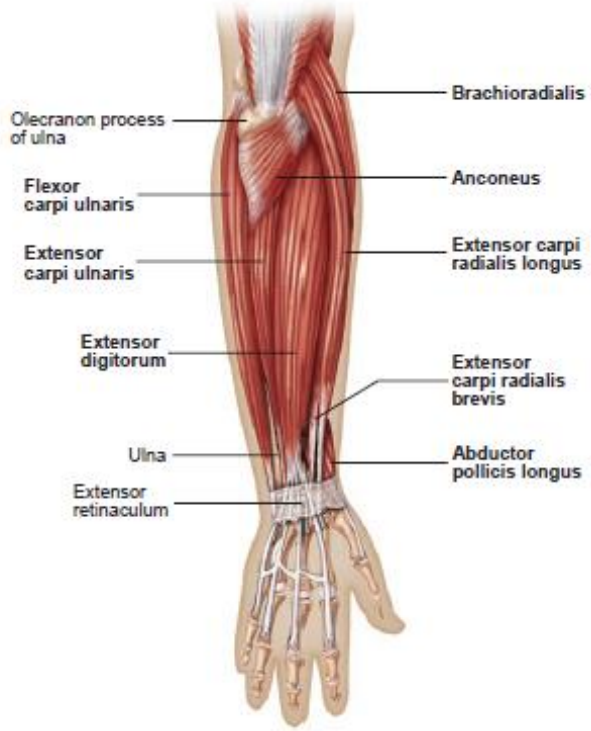

Figure 2.2: Posterior view of the right forearm superficial muscles [16]

2.2 SURFACE ELECTROMYOGRAPHY

Electromyography is the study of the electrical signals generated by the muscles. These signals are rich in information about the functionality from the muscle and can be exploited for the control of myoelectric prosthesis. But before examining this electrical signal, it is relevant to understand how they are generated in the human body.

2.2.1 Muscle Physiology and sEMG signal

Action potentials are the electrical signals that originate the muscle contraction. The action potential is generated due to the capability of nerve cell membranes to allow the passage of Na^+ ions and K^+ ions. These signals are propagated from the brain or spinal cord along axons of nerve cells to skeletal muscle fibers and causes them to contract.

Plasma membranes are polarized, which means there is a voltage difference across each plasma membrane. The voltage difference of an unstimulated cell is called the resting membrane potential, which is typically about -85 mV. However, stimulation of a cell can cause depolarization of its plasma membrane. If the depolarization makes the membrane potential reach a value called “threshold”, an action potential is triggered. An action potential, typically takes about 1 millisecond to a few milliseconds to occur and it is constituted by two phases: depolarization and repolarization. During the depolarization phase, the inside of the cell becomes positively charged after cell stimulation because of the opening of Na^+ channels present in the membrane. These positively charged ions make the inside of

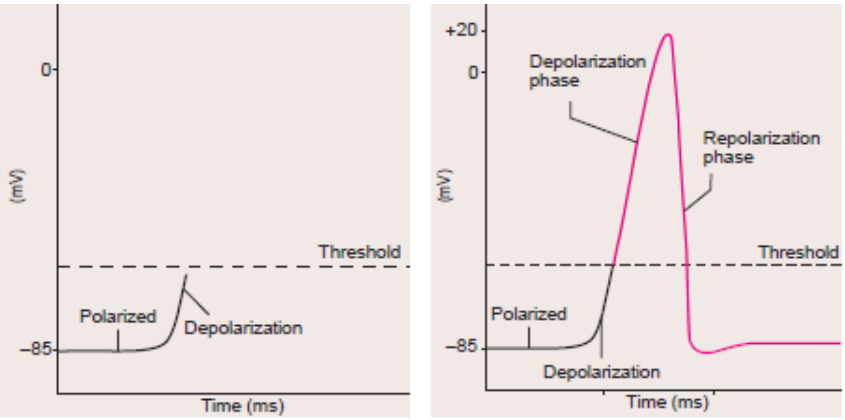

Figure 2.3: On the left: Voltage difference across the plasma membrane on the beginning of the depolarization phase; On the right: Voltage difference during and after the action potential. [16]

the cell less negative and, if the threshold value is reached, more voltage-gated Na^+ channels will open rapidly, making the inside of the membrane positive for a brief time (about +20 mV). This voltage change causes additional permeability changes in the plasma membrane, which makes depolarization to stop and repolarization to start. During this phase, the Na^+ channels close and the movement of K^+ to the exterior of the cell increases, making the inside of the plasma membrane to become more negative and the outside more positive. After the resting membrane potential is reestablished, voltage-gated K^+ channels close and the action potential ends. The generation of an action potential, therefore depends if the stimulus is strong enough to reach the threshold value and cause depolarization. This is called the all-or-nothing principle.

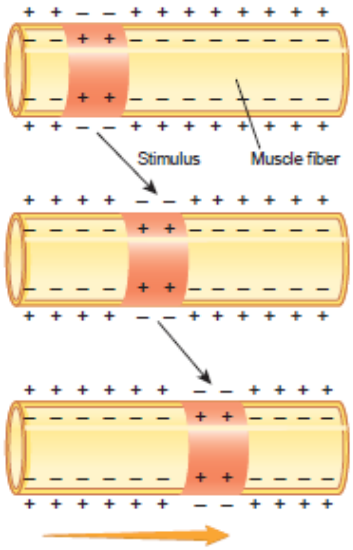

Figure 2.4: Propagation of an action potential across a muscle fiber. [16]

Although an action potential occurs in a very small area of the plasma membrane, it can propagate across it by stimulating the generation of another action potential in an adjacent location, which also generates another action potential, and so on. This is illustrated in Figure 2.4. Action potentials that are carried by motor axons cause another action potentials to be produced in muscle fibers, causing cross-bridge movement and muscle sarcomere contraction [16].

The motor unit is the basis of skeletal muscle. It consists of a single motor neuron and the group of skeletal muscle fibers to which is attached. The motor unit is the smallest unit that can be activated by a volitional effort, which means all the muscle fibers that are part of it are activated synchronously.

The evoked field potential from a Single Motor Unit (SMU) has a duration of 3 to 15 ms and an amplitude of 20 to 2000 μV, depending on the size of the motor unit. One of the downsides of using sEMG sensors is that they are sensitive to electrical activity over an area too wide. In Figure 2.5 it is possible to observe the *normal dorsal interosseous* muscle under different degrees of contraction. In a low level of contraction, it is possible to differentiate the potentials from different SMUs, but as the level of contraction rises, active SMUs increase their firing rate and new ones are recruited, making individual SMUs no longer distinguishable in the EMG signal [17].

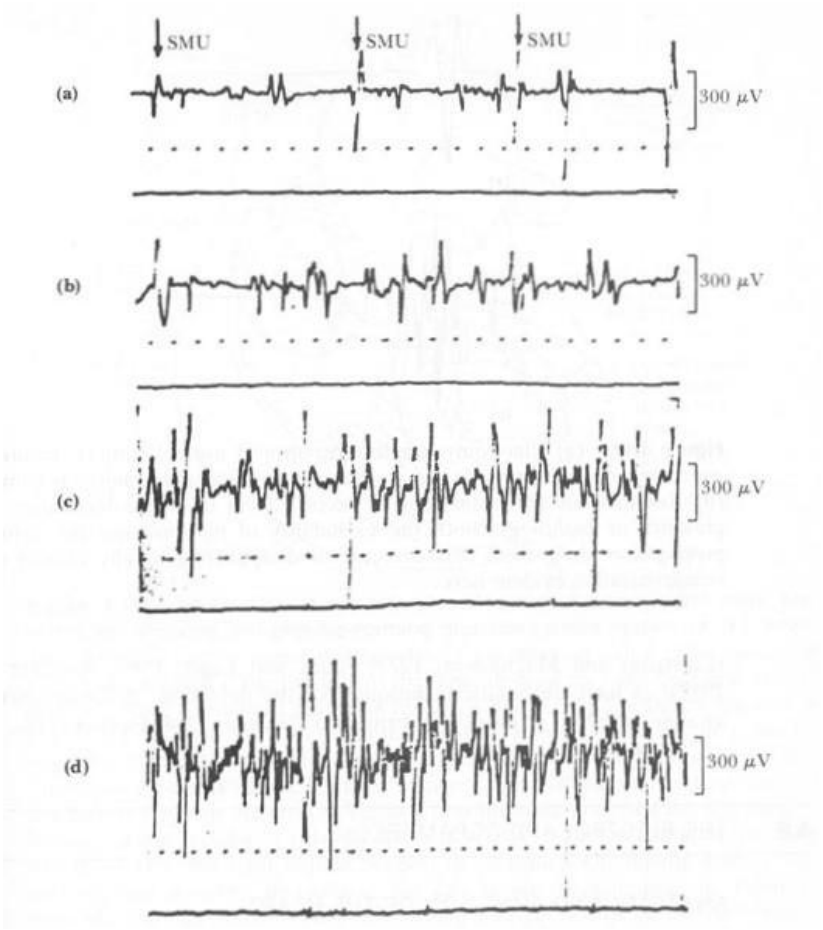

Figure 2.5: *Normal dorsal interosseous* muscle under different degrees of contraction. The degree of contraction increases from (a) to (d). Time scale is 10 ms per dot. [17]

sEMG uses non-invasive surface electrodes, which are placed directly on the skin surface and can detect the sum of the signals generated by SMUs. Its main advantage is the non-invasiveness, making this method of easy application and non-painful for the patient. The main disadvantage is, as mentioned above, the difficulty in distinguishing SMUs from each other in the sEMG signal.

2.2.2 State of the art

Due to all the advantages of sEMG mentioned in the previous section, this method has been applied successfully in diverse research areas. For instance, in therapeutic use, the usage of a sEMG system where the subject has visual feedback can have positive effects on reducing the level of PLP [18] [19]. According to the work of L. Nikolajsen and T.S. Jensen [6], cortical reorganization after amputation is a factor that might be related to the origin of the PLP and it is based on the remark that

the success of the usage of sEMG control systems with visual feedback as treatment for this condition can be explained.

A.L. Alphonso et al. [18] used sEMG signals to control a 3D limb in a virtual integration environment. After 20 days of virtual therapy with wrist movements and different hand gestures, the data acquired from 18 transradial and transhumeral amputees showed a reduction of PLP level. M. Ortiz-Catalan et al. [19] tried a more innovative solution by using augmented reality and gaming. The myoelectric signals from a transradial amputee's residual limb were used to control a virtual limb, along with a computer game controlled by phantom wrist movements. Over the course of 18 weeks, the pain level gradually decreased to long painless periods. On the other hand, C. Dietrich et al. [20] showed that prosthesis functionality can be increased and PLP reduced with the use of a prosthetic hand with somatosensorial feedback on grip strength.

Systems that use sEMG for the teleoperation of a robotic arm are also a target for research and can have several applications, such as remote surgeries [21] and as a personal assistant of desktop work for forearm amputees [22]. Another application for sEMG can be the control of an arm exoskeleton, which is a supporting structure on the outside of a body that aids movement. K. Kiguchi and Y. Hayashi [23] successfully applied an exoskeleton to the right arm in their work. With the use of the exoskeleton, controlled by the EMG signals from the upper limb, it was possible to amplify the power of the strength applied. This way, the exoskeleton could assist in bearing a heavier load in the hand, along with helping the forearm in its natural movement. Besides, the use of sEMG-driven exoskeletons has also application in the rehabilitation area, as seen in the work of M. Mulas et al. [24], where the signals from sensors placed on the forearm helped move a hand exoskeleton for people who lost the ability of moving correctly the hand musculature, due to a stroke or spinal cord injuries.

Beside physical tasks, sEMG control systems can also have an important role to play in communication. For example, V.E. Kosmidou and L.J. Hadjileontiadis [25] have successfully identified 60 Greek Sign Language hand signs by combining sEMG data from the forearm with accelerometer data, acquiring more than 93% of accuracy.

Between the wide range of applications for this bio-signal, the usage of sEMG for the control of myoelectrical prostheses is the most active research area. For the context of this work, sEMG hand-gesture classification for transradial prosthesis control will be the focus. Since the work by B. Hudgins et al. [26], where the use of pattern recognition techniques and of sEMG signals was applied to prosthetic control, lots of studies were published using different methods and different machine learning algorithms with positive outcome, as observed in the work of F. Tenore et al. [27], where different finger movements try to be recognized with the use of 32 sEMG electrodes on able-bodied subjects. It is also important to reduce the number of sensors without compromising the accuracy of the system, like in the work of G.R. Naik et al. [28] where various gestures were identified using the minimum number of sensors, selected with the use of a method called Independent Component Analysis. This method was validated on 5 transradial amputees. The recognition of the hand gestures can be done after data is acquired but also in real-time, as seen, in the work of C. Cipriani et al. [29], where eight pairs of electrodes were placed on the residual limbs from 5 transradial amputees and forearms of 5 able-bodied subjects to control a robotic hand with the use of seven finger movements. A 79% accuracy was obtained for the amputees and 89% for healthy subjects, which also indicates that is relevant to make statistical analysis to compare data from able-bodied subjects with the data from amputees. Beside these examples, there are much more, like the works from R. Ahsan et al. [30], F. Riillo et al. [31] and X. Jiang et al. [32], making it evident that sEMG has a higher application to hand gesture recognition and myoelectric prosthesis than in other areas, as it is shown in Table 2.1.

Table 2.1: Used references and respective applications of the sEMG signal

Reference	Application
A.L. Alphonso et al. (2012)	PLP treatment
M. Ortiz-Catalan et al. (2014)	PLP treatment, gaming
C. Dietrich et al. (2012)	PLP treatment, myoelectric prostheses
J. Vogel et al. (2011)	Teleoperation, control of robotic arm
O. Fukuda et al. (2013)	Teleoperation, control of robotic arm
K. Kiguchi and Y. Hayashi (2012)	Exoskeleton, Rehabilitation
M. Mulas et al. (2005)	Exoskeleton, Rehabilitation
V.E. Kosmidou and L.J. Hadjileontiadis (2009)	Sign Language, hand gesture recognition
F. Tenore et al. (2007)	Myoelectric prostheses, hand gesture recognition
G.R. Naik et al. (2015)	Myoelectric prostheses, hand gesture recognition
C. Cipriani et al. (2011)	Myoelectric prostheses, hand gesture recognition
R. Ahsan et al. (2011)	Myoelectric prostheses, hand gesture recognition
F. Riillo et al. (2014)	Myoelectric prostheses, hand gesture recognition
X. Jiang et al. (2017)	Myoelectric prostheses, hand gesture recognition

There are already several multi-finger active myoelectric prostheses available commercially, like the Touch Bionics i-Limb, RSL Steeper BeBionics 3 and OttoBock's Michelangelo Hand [12]. As mentioned before, the price of existing myoelectric prostheses continues to be a problem for the final user. However, there are some efforts being made to produce low-cost myoelectric prosthesis, like the usage of 3D printed components to reduce production price.

P. Slade et al. [33] built an open-source, 3D printed myoelectric prosthetic hand with the cost of just $250. Another 3D printed hand for the usage of transradial amputees was built by K.F. Gretsch et al. [34]. with the cost of $300. It is shoulder controlled and the user can open and close all five fingers, and move the thumb independently. M. Polisiero et al. [35], on the other hand, built a one degree-of-freedom myoelectric prosthetic hand for amputees living in developing countries using a light aluminium structure that acts as a clamp, powered by a DC motor, that has the only one functionality: grasping. The cost of the electronic and mechanical components to build this prosthesis was $50. Even the Myo Armband, a commercial low-cost device for gesture control that features eight sEMG sensors, has been used, with success, for the real-time control of a myoelectric prosthesis [36].

Besides all the possible applications of sEMG on prosthetics, there are currently other bio-signals that have the potential to control a robotic prosthesis, like non-invasive techniques such as force myography [32], ultrasound imaging [37], optical myography [38], or invasive techniques such as implantable myoelectric sensors or neural interfaces [4].

2.2.3 Myoelectric Control System

The typical control strategy for most of the commercial myoelectric prosthesis available is based on the rectified Mean Absolute Value (MAV) from the sEMG signal. The MAV increases and decreases according to the level of muscle contraction of the user. When the MAV is below a threshold level, the prosthetic hand will perform one action (i.e. open hand), and when above, the prosthetic hand will perform a different action (i.e close hand) [39]. This type of system control is very limited because it only allows one kind of movement, which is normally the closing and opening of the hand to grasp

objects. Although this control method is used in a wide variety of prostheses, the focus of this work will fall on myoelectric control with pattern recognition which offers much more interesting possibilities.

The usage of pattern recognition techniques in myoelectric prosthetic control systems relies on the usage of machine learning algorithms, called classifiers, that can recognize patterns in the sEMG signal and give them a class label that corresponds to a certain movement or gesture. This process is called classification. The fundamental steps behind myoelectric control are schematized in Figure 2.6.

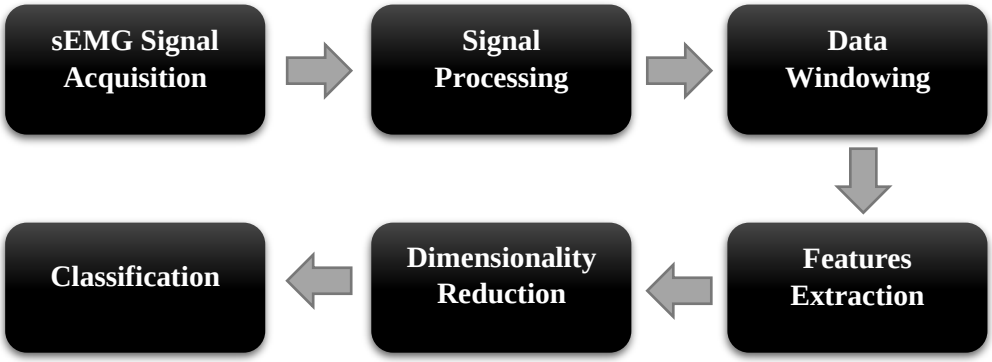

Figure 2.6: The fundamental steps of myoelectric control (inspired by [41])

During signal processing, all the unwanted noise is removed from the EMG signal, which is very noisy by nature due to several reasons such as the inherent noise from the electrodes, internal noise, electromagnetic noise, inherent instability of the signal, ECG artefacts and unwanted EMG signals from other muscular groups [40]. During this stage, other processing techniques can be applied to the signal, such as downsampling or applying an envelope to the signal, changing the original signal, which can originate better results later, on the classification phase. Next, the signal should be separated in windows, a process that is called “data windowing”. Each of these windows will be given a class label.

The next step is the feature extraction from each window. Feature is the name given to any relevant characteristic that can be extracted from the signal, such as the mean, energy, wavelength, etc. The chosen window length must be taken into consideration because the bigger the selected length is, the higher the stability of the selected features, reducing the variance and increasing classification performance. However, the increased window length will also increase the time of classification decision. The results from a real-time control test suggested the optimum window length is between 150 and 250 ms, depending on the subject’s skill [41].

An increased window length can originate feature vectors with high dimensionality, which can be a problem for classification. Because of this issue, it might be necessary to complement the feature extraction with dimensionality reduction techniques, such as principal component analysis or common spatial pattern [31]. These kinds of methods decrease the burden of the classifier, along with the computational time. However, this type of techniques was not used in the work described in this dissertation

Finally, the feature vectors are given as input to the classifier, which will decide to which class the given feature vectors belong to. The calculated class label will influence the action taken by the actuator, which can be, for example, a prosthetic hand. The class can correspond to a certain hand gesture, a type of movement, a grip force level, etc. A detailed explanation of machine learning algorithms for pattern recognition will be presented in the following sub-chapter.

2.3 PATTERN RECOGNITION ALGORITHMS

A classifier is a pattern recognition algorithm whose purpose is to automatically estimate a class for a feature vector. First, the classifier must be trained with a set of data containing observations whose classes are known, called training set. With the information extracted from the training set, the classifier should be able to categorize data whose observation classes are unknown. This set of data is called testing set. Therefore, classification is divided in two phases: training and testing. It is also relevant to understand that the performance of pattern recognition depends on both feature extraction and the classification algorithm employed.

Classification is a problem that belongs to statistical and machine learning areas. These algorithms have a broad range of applications (e.g. autonomous robotics, knowledge discovery, myoelectric prosthesis or computational economics [42]) and there are numerous different types and variations. However, the main algorithms used in this work were the Linear Discriminant Analysis, which does not feature automatic learning, along with the Support Vector Machine (SVM), naïve Bayes and *k* Nearest Neighbours (kNN), which all feature automatic learning. These classifiers are described thoroughly in the following sections.

2.3.1 Linear Discriminant Analysis

LDA is a linear classifier that is based on the use of hyperplanes to separate data that contains different classes. For example, as it can be observed on Figure 2.7, the hyperplane tries to separate the features belonging to the “crosses” class from the “circles” class. The class given to a certain feature depends on which side of the hyperplane is located. In this example, it is possible to observe that one “cross” and one “circle” were misclassified.

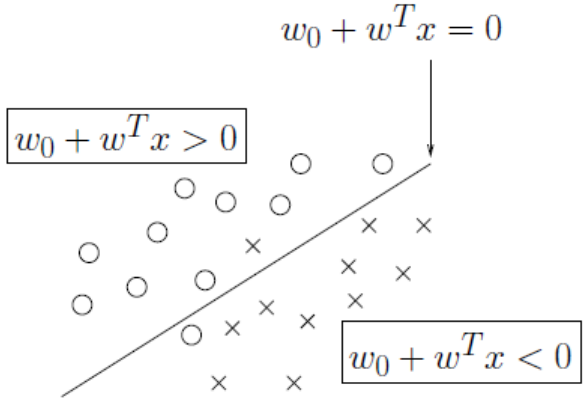

Figure 2.7: A hyperplane that separates two classes, the "crosses" and the "circles" [43].

It is assumed that the data follows a normal distribution and with an equal covariance matrix for both classes. The covariance matrix is a matrix where the element in the *i, j* position is the covariance between the i^{th} and j^{th} elements from the feature vector. To acquire the optimal hyperplane, it is necessary to find the projection that maximizes the distances between both the means from both classes and minimizes the interclass variance. To solve a classification problem with more than two classes, several hyperplanes must be used [43].

Considering an input feature vector x, with $x_i \in R^n$, $i = 1,2, \dots N$, n being the total number of features and R the feature space, a hyperplane in R^n can be represented as $\boldsymbol{w}^t x + w_0 = 0$, where $\boldsymbol{w} \in R^n$ is a n-dimensional vector and w_0 is a constant. Assuming x_i belongs to class A or B, LDA's objective is to find optimal values for $\boldsymbol{w}$ and w_0, in a way that:

$$\boldsymbol{w}^t x_i + w_0 > 0 \; if \; x_i \; belongs \; to \; class \; A \quad (2.1)$$

$$\boldsymbol{w}^t x_i + w_0 < 0 \; if \; x_i \; belongs \; to \; class \; B \quad (2.2)$$

When $\boldsymbol{w}^t x + w_0 = 0$, the class is typically given in an arbitrary way.

The main advantages of this technique fall on the fact that it is a classifier of relative easy implementation and easy to train. It also offers computational efficacy, which allows a good real-time performance. The main downside of LDA is that, due to its linearity, it can return poor results when applied to problems with non-linear, complex data, such as sEMG. Despite this disadvantage, LDA has generated good results when classifying data for hand-gesture recognition, such as in F. Riillo et al. [31], where it achieved a maximum average accuracy of 86.49% for able bodied-subject and 92.16% for one amputee. Also in X. Jiang et al. [32], the results were quite satisfying, achieving a classification accuracy of 84.60%.

2.3.2 Support Vector Machines

Much like the LDA, the SVM algorithm also makes use of hyperplanes to identify different classes. However, SVM makes sure to find the hyperplane that has the maximum margin from both classes, i.e., the distance from the nearest training points [43]. In Figure 2.8 is depicted a binary classification problem similar to the one approached in the previous section, where the "circles" belong to class *A* and the "crosses" belong to class *B*.

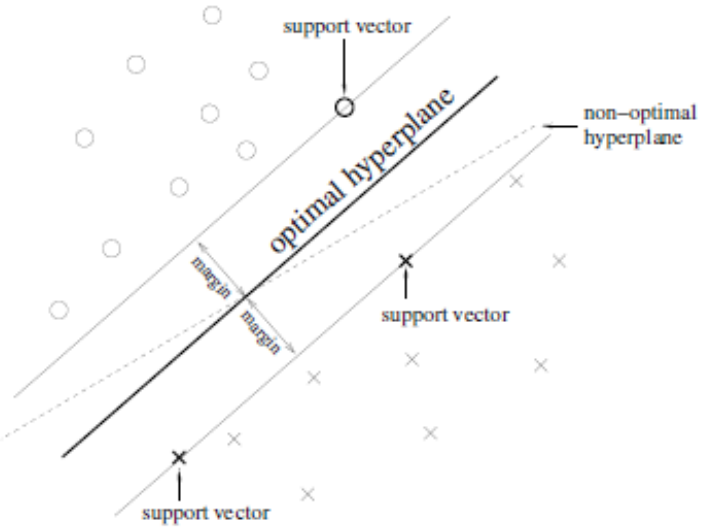

Figure 2.8: SVM finds the optimal hyperplane that has the maximum margin from both classes [43]

At first sight, the separation between the two classes can be made by any line that divides the regions containing only "crosses" and only "circles". Intuitively, the dark line seems to provide a better decision boundary than the dashed line, because it appears to have a bigger safety margin. On this binary classification problem, the SVM algorithm is used to find the hyperplane that provides the maximum

distance from both classes, which in this case is the dark line from Figure 2.8. The points closer to the hyperplane are called "support vectors", on which ***w***, the weight vector, depends. This hyperplane may have a dimension higher than the number of features. Given ***w***, it is possible to calculate w_0. The maximization of the margin is acquired by minimizing the norm of ***w***, called the "objective function":

$$J(\boldsymbol{w}) = \frac{1}{2}\boldsymbol{w} \cdot \boldsymbol{w} \quad (2.3)$$

In the SVM's case, contrarily to the LDA, it is necessary that the training patterns lie on the right side of the decision boundary, while considering the safety margin, as mentioned above. Therefore, during the training phase, stricter inequalities are required, such as:

$$\boldsymbol{w}^t x_i + w_0 \geq 1 \; if \; x_i \; belongs \; to \; class \; A \quad (2.4)$$

$$\boldsymbol{w}^t x_i + w_0 \leq -1 \; if \; x_i \; belongs \; to \; class \; B \quad (2.5)$$

Finally, during the testing phase, the usual rules are applied (expressions 2.1 and 2.2). This optimization problem can be put in terms of a convex quadratic program and it can be solved by well-known techniques [44]. One of these techniques is called Sequential Minimal Optimization, or SMO. This algorithm breaks this large Quadratic Programming (QP) optimization problem into a series of smaller QP problems, as smallest as possible. These problems are solved analytically, avoiding QP optimization as an inner loop, which is too time-consuming. SMO is therefore a very fast algorithm for training SVMs and allows the handling of very large training sets [45].

2.3.2.1 The Soft-Margin Implementation

The training strategy presented in the previous section can, however, fail if the data is not linearly separable. In this situation, one of the possible solutions could be based on finding a hyperplane that leads to the minimum possible error. There are two kinds of error to consider in this situation: the feature vectors that are on the wrong side of the hyperplane and the ones which are on the right side, but within the safety margin. In other words, the misclassifications and correct classifications with insufficient certainty. Therefore, the problem can be modeled by the following inequalities:

$$\boldsymbol{w}^t x_i + w_0 > 1 - \xi_i \; if \; x_i \; belongs \; to \; class \; A \quad (2.6)$$

$$\boldsymbol{w}^t x_i + w_0 < -1 + \xi_i \; if \; x_i \; belongs \; to \; class \; B \quad (2.7)$$

Where the "slack variable", ξ_i, is the associated error for each training instance, x_i.

The sum of all the errors is then added to the objective function, along with a regularization parameter *C*:

$$J(\boldsymbol{w}, \xi) = \frac{1}{2}\boldsymbol{w} \cdot \boldsymbol{w} + C\left(\sum_{i=1}^{N} \xi_i\right) \quad (2.8)$$

Where *C* is added to weight the sum of the errors. This parameter allows a trade-off between training set accuracy and expected generalization capability. A large value of *C* will originate a hyperplane that commits fewer errors on training data but will have a smaller safety margin, thus less expected generalization. On the other hand, a small value of *C* will allow more errors on training data, but the safety margin will be wider.

This is called the soft-margin implementation and its usage can be very benefic for EMG data, because of its complexity and high number of outliers.

2.3.2.2 The Kernel Function

It is also possible to create non-linear decision boundaries with a small increase in the SVM's complexity, using a Kernel function. To help understand this method, Figure 2.9 should be observed. The black circles correspond to class A and the white circles to class B. The data set is bi-dimensional and it is not separable in a linear way. However, when the data is projected in a tri-dimensional space, it becomes easy to separate both classes with the use of a plane.

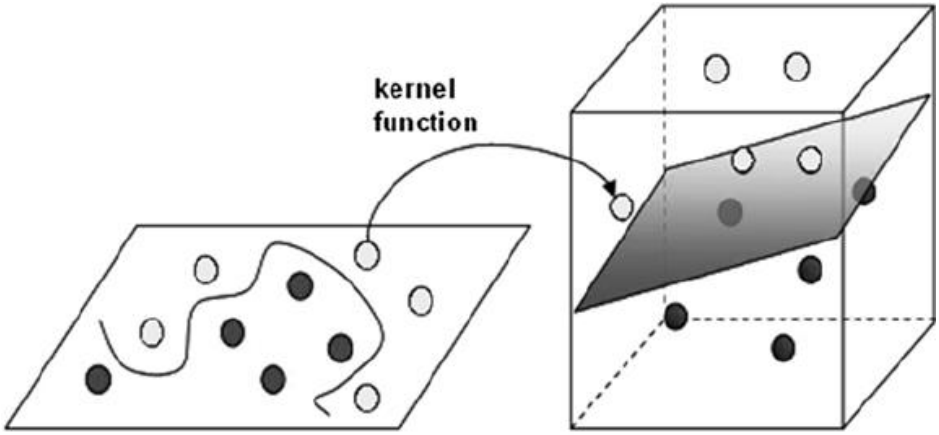

Figure 2.9: The data set is not linearly separable in bi-dimensional space. However, in tri-dimensional space, it is easily separable (adapted from [46]).

Despite the simplicity of this example, it is easy to understand that when data is not linearly separable in its original space, it can be so if projected in another space, especially if the dimensionality is higher.

Considering that $\varphi: R^n \rightarrow H$, $\varphi(x_i)$, represents the projection of the input x_i in another space. The training algorithm depends of $\varphi(\cdot)$ only through the scalar product between the projected instances $\varphi(x_i) \cdot \varphi(x_j)$. There is a function $K: R^n \times R^n \rightarrow R$, where $K(x_i,x_j) = \varphi(x_i) \cdot \varphi(x_j)$, that avoids the need the explicit mapping of both $\varphi(x_i)$ e $\varphi(x_j)$ functions, making the usage of K sufficient in the training algorithm. K is known as the Kernel function. To be valid, this function requires symmetry, such that $K(x_i,x_j) = K(x_j,x_i)$. It is also necessary that reflects similarity between the output, if both inputs are similar, then it is expected for K to have a high value. Some of the most used Kernels include the following [47]:

- Polynomial (the parameter q is previously selected):

$$K(x_i, x_j) = ({x_i}^T x_j + 1)^q, q > 0 \quad (2.9)$$

- Radial-basis function (the parameter r is previously selected):

$$K(x_i, x_j) = exp\left(-\frac{\|x_i - x_j\|^2}{2r^2}\right), r \neq 0 \quad (2.10)$$

- Sigmoidal functions:

$$K(x_i, x_j) = tanh(2{x_i}^T x_j + 1) \quad (2.11)$$

The SVM are known for having good generalization properties, to be insensitive to overfitting and to the "curse of dimensionality". Both concepts will be explained in the section 2.3.4. Such advantages have allowed the SVM to become very popular in sEMG application and it has produced good results for hand gesture classification, as seen in F. Riillo et al. [31]. Due to its high use in research, the SVM has several variations that can be useful for specific problems.

2.3.3 Bayes Classifier

In classification, the Bayes rule can be used to calculate the probabilities of the classes. Bayes rule provides a decomposition of a conditional probability that is frequently used in a family of learning techniques, called "Bayesian learning" Algorithms that use this rule classify an input feature vector *x* according to the probability to which class is more likely to belong to [47]. The Bayes rule is described by the following equality:

$$P(A|x) = \frac{P(x|A) \cdot P(A)}{P(x)} \quad (2.12)$$

Where *P(A|x)* is the probability that the input vector *x* belongs to class *A*, *P(x|A)* is the conditional probability of the input feature vector considering it belongs to class *A*, *P(A)* is the a-priori probability of class A and *P(x)* is the a-priori probability of the input feature vector.

Considering the binary classification problem once again, with class *A* and class *B*, if *P(A|x)>P(B|x)*, then the input feature vector belongs to class *A*, otherwise, if *P(A|x)<P(B|x)*, then the input vector belongs to class *B*.

2.3.3.1 Naïve Bayes

The Naïve Bayes, also known as Idiot's Bayes, is a relatively simple learning algorithm that uses the Bayes rule, assuming the features are conditionally independent, given the class. Such assumption entitles:

$$P(x|y) = \prod_{i=1}^{n} P(x_i|y) \quad (2.13)$$

Where x_i is the value of the i^{th} attribute of *x*, *y* is the class label (for the binary classification considered above, *y* can be equal to A or B) and *n* is the number of attributes. *P(x)* can also be calculated by using:

$$P(x) = \prod_{i=1}^{k} P(y_i) P(x|y_i) \quad (2.14)$$

Where k is the number of classes and y_i is the i^{th} class. Therefore, the equality 2.12 can be solved by using expressions 2.13 and 2.14, normalizing the numerators on the right side of the equation [48].

The simplicity of Naïve Bayes provides many advantages, such as computational efficiency, incremental learning and robustness in the face of noise and in the face of missing values. However, since it provides low variance, the bias value is high (see section 2.3.5.3 about the bias-variance trade-off). Because of these desirable characteristics, naïve Bayes is used for many applications, which includes hand-gesture classification. In the work by J. Wu et al. [49], the naïve Bayes was used for American sign language recognition using sEMG sensors combined with inertial sensors. This classifier calculated a maximum accuracy of 84.11%.

2.3.4 *k* Nearest Neighbours

The nearest neighbour classifiers are relatively simple to understand and implement. These algorithms consist in assigning a feature vector to a class, according to its nearest neighbours. In a data set S, the nearest neighbour to a data object q is the data object S_i, which minimizes $d(q,S_i)$. The function d represents a *distance measure* defined for the object in question [48].

The k Nearest Neighbours (kNN) aims to assign the dominant class to an object among its k nearest neighbours within the training set. If the selected k value is high enough and there are enough training samples, kNN can approximate any function, enabling this classifier to generate non-linear decision boundaries [43].

The kNN algorithm is very sensitive to the "curse of dimensionality", which is described in section 2.3.5.1. However, in the work by J. Wu et al. [49] referred in the previous section, it was calculated a maximum accuracy of 98.56%, higher than the naïve Bayes classifier.

2.3.5 Main Classification Problems

Signals from sEMG are known for being non-stationary, having an increased number of outliers, high-dimensional features and a high amount of noise. These inherent signal characteristics can originate some issues for the classification process. Some of the most relevant problems are described in this section.

2.3.5.1 The Curse of Dimensionality

The higher the dimensionality of the feature vectors, the higher is the amount of data required to properly describe different classes. If the data from the training set is too small, relatively to the size of the features, then, probably, the classification results will be unsatisfying. According to F. Lotte et al. [43], it is recommended to use, at least, five to ten times as many training samples per class as dimensionality. In the sEMG case, the dimensionality is high, and the training sets are generally small, making this curse a major issue in classification using this type of electrical signals. There are several methods for reducing the effects caused by the curse of dimensionality, like feature selection and dimensionality reduction. However, there is no single solution for the issues caused by it [48].

2.3.5.2 Overfitting

If there is too much noise in the data for classification, an overcomplex hypothesis may learn not the underlying function but also the noise and may make a bad fit. For example, if the noisy data from a third-order polynomial was fitted by a sixth-order polynomial. This is called overfitting. For better understanding, an example is illustrated in Figure 2.10.

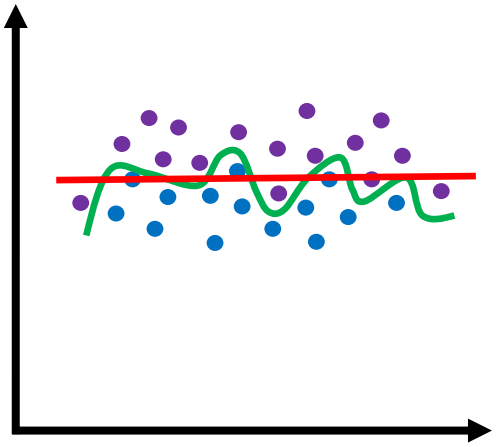

Figure 2.10: Example of overfitting. The green line represents an overfitted model, the red line represents a regularized model and the blue and purple dots are two different classes from the training data.

The green line represents an overfitted model, the red line represents a regularized model and the blue and purple dots represent two classes from the training data. At first sight, the overfitted model seems to provide better results, since the line that best separates both classes from the training data is the green one. However, the overfitted model is too dependent on it and, when confronted with new training data, it is more probable to occur errors. On the other hand, the red line would provide better results in the long term. Overall, an overfitted model has a low predictive performance and overreacts to minor fluctuations in the testing data. However, having more training data helps to overcome this issue, but only to a certain point [44]. Moreover, simpler algorithms, like LDA, are more unlikely to overfit data.

2.3.5.3 The Bias-Variance Trade-off

Let $\boldsymbol{x}$ be the input feature vector and y and corresponding class label, and let $f = f(\boldsymbol{x})$ be an estimator of y. It is possible to measure how different is the estimation from the true class label and evaluate the quality of the estimator. Because it is a random variable, the Mean Square Error of the estimator, $MSE(f, y)$, must be considered:

$$MSE(f, y) = E[(f(\boldsymbol{x}) - y)^2] \quad (2.15)$$

The bias represents the divergence between an estimation of the class label and the true class label. The bias of the estimator is defined as:

$$b_y(f) = E[f(\boldsymbol{x})] - y \quad (2.16)$$

Therefore, equation 2.15 can be rewritten as it follows, where f is $f(x)$ [44]:

$$MSE(f, y) = E[(f - E[f])^2] + (E[f] - y)^2 + 2(E[f] - y)E[(f - E[f])] \quad (2.17)$$

Because *E[f] - y* is a constant and *E[f – E[f]] = E[f] – E[f] = 0*, equation 2.17 becomes:

$$E[(f - E[f])^2] + (E[f] - y)^2$$

The first term from equation 2.17 is the variance of ***f(x)***, *Var(f)*, and the second is the square of the bias, therefore we have:

$$Var(y) + [b_y(f)]^2$$

Variance measures how much, on average, ***f(x)*** varies around the expected value, which means that it reflects the sensitivity to the training set used.

Therefore, to acquire the lowest classification error, both the bias and variance should be low. Unfortunately, there is a "natural" trade-off between bias and variance. Stable classifiers tend to have high bias and low variance while, on the other hand, unstable classifiers have low bias and high variance. Perhaps this could be the reason why simple classifiers can, sometimes, outperform more complex ones.

Because EMG signals are non-stationary, training sets from different sessions are probably different between each other. A classification with low variance can be a solution to deal with this variability problem. To reduce it, some methods like combination of classifiers or regularization can be used [43].

2.3.6 Classification Performance Evaluation

The performance of a classifier is usually evaluated using the accuracy, which is defined as the number of correctly classified instances over the total of instances. It also can be evaluated using the error rate, which, contrarily to accuracy, is defined as the number of incorrectly classified instances over the total of instances. There are different methods used to evaluate accuracy:

- **Train-Test evaluation**: the whole data-set is split into a training set and a testing set, which can be done in random or sequential order. The calculated accuracy is based on the classification results from the testing set.
- ***k*-fold cross validation**: the data from the whole data set is split into *k* subsets, of approximately same size, S_1, …, S_k each called a fold. The learning algorithm is then applied *k* times, for *i=1* to *k*. In each iteration the union of all *k-1* subsets, other than S_i, is set as the training set and S_i as the test set [48]. The final accuracy is the average of the accuracies obtained for each iteration.
- **Leave-one-out cross validation:** it is a special case of cross validation where the number of instances of the data set is equal to the number of folds. The learning algorithm is applied once for each instance, while using all the other instances as training set and using the one left out as testing set [48].

Computationally speaking, cross validation is much more demanding than the train-test evaluation, since it uses a higher amount of data of training. The advantage is that all the data is used at least once for testing, which allows to have an unbiased performance estimate.

Sometimes it is also necessary to compare accuracies from different classifiers or the classification results from different sessions. For this, it is possible to use statistical tests, such as variance analysis, Friedman's test, Wilcoxon signed rank test or Student's t-test.

3 MATERIALS

As stated in the beginning of this document, two separate systems will be used to make sEMG measurements on both amputated and able-bodied subjects. One of these systems uses low-cost sensors and the other high-end ones. The acquired sEMG data will be used for hand gesture classification and the results from both systems will be compared. The main objective is to investigate if the classification accuracy calculated with the low-cost sensors can be equal or even superior than the accuracy calculated with the usage of the high-end sensors. To do this, different combinations of signal processing techniques and classifiers were tested to obtain the best results possible.

Two experiments were designed to acquire sEMG data, the first experiment was done on able-bodied subjects to check if the results were promising enough before moving on and doing further measurements on amputated patients. The second experiment was done on transradial amputees and in able-bodied subjects, using an optimized protocol and a higher number of sensors. Besides, a few modifications based on observations from the first experiment were applied.

Both experiments were performed using two different measuring systems: the Myo Armband and a system built with sensors from OttoBock, which are both described thoroughly in the following sections.

3.1 THE OTTOBOCK SYSTEM

"OttoBock system" was the name given to the system that uses OttoBock sensors. The sensor model chosen was the Otto Bock MyoBock 13E200=50, which are the standard electrodes used for clinical prosthetic applications. The first step was to understand the sensor's specifications. Some of them can be found in the manufacturer's catalogue [15] and are represented in Table 3.1.

Table 3.1: Specifications from Otto Bock MyoBock 13E200=50 [15]

Weight	4.5g
Frequency	50 Hz
Operating voltage	4.8-7.2V
Dimensions (L×W×H)	27 × 18 × 9.5 mm
Frequency bandwidth	90 to 450 Hz
Ambient temperature	-15 to +60 degrees C

Furthermore, these sensors provide adjustable sensitivity (2,000-100,000×, level 1 to 7) [50], onboard rectification and band pass filtering, to provide a high-quality signal [8]. These electrodes are differential, which means that they have three terminals and can acquire sEMG signals without any other reference signal. The output voltage from the sensor is between 0 and 5V and the signal is already enveloped. The input voltage for the sensors was set to 7.2V.

The sensors were interfaced with an Arduino Leonardo microcontroller. An Arduino was chosen for this task because it offers an easy interface with the computer, its *firmware* is simple to write due to many dedicated functions and it is cheap. Arduino Leonardo features a 10-bit Analog-to-Digital

Converter (ADC) and 6 analog channels. The recommended input for each analog channel is 5V, which is perfect, considering the sensor's output.

Between the first and second experiment, due to availability reasons, the number of OttoBock sensors was different and, therefore, while general considerations for the two experimental setups are similar, in the following sections some differences must be considered. Moreover, in order to have a consistent comparison with the Myo system, only the signals acquired from correspondent positions of the sensors were considered for data analysis.

3.1.1 Setup 1: five OttoBock sensors configuration

The setup 1 was used for the first experiment. In this setup, five OttoBock sensors were used. The sensors were interfaced directly with the Arduino, which can acquire data with a 10-bit resolution, as stated above. According to Nyquist Theorem, the sampling rate of a signal should be at least twice its frequency [51]. Because the frequency bandwidth listed in the sensor's specifications is 90-450Hz, the selected sampling rate was set to 1KHz, which is higher than the double of 450Hz.

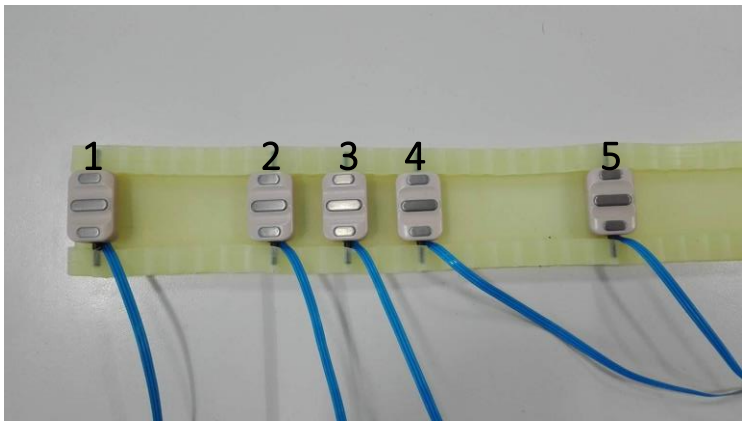

Figure 3.1: The OttoBock sensors enclosed in the silicon band according to setup 1. The numbers given to the sensors match the ones given to the ones from the Myo Armband in setup 1

All the five OttoBock sensors were enclosed into a silicon band (manufactured at INAL) and a number was given to each of them, 1 to 5, as shown in Figure 3.1. This sequence is supposed to be analogous to the one given in setup 1 from the Myo system, where the sensors are also numbered from 1 to 5. When placed on the forearm, the sensors from both systems that have the same number, should be placed on the same position.

3.1.2 Setup 2: eight OttoBock sensors configuration

This setup was used for the second experiment. To match the same number as the Myo Armband, eight OttoBock sensors were used. Because of the increased number of sensors, some changes to the system were necessary. As referenced above, Arduino Leonardo only features six analog channels. To overcome this problem, an 8-channel external ADC was used to make possible the data acquisition: the acquired digitalized data from the ADC is transferred to Arduino whose function in this case is the interface with the computer. The selected ADC was the MCP3304 by Microchip [52] which features a

12-bit resolution. The sampling frequency was also changed to 500Hz, which has been proved to be enough for gesture recognition [53]. By reducing the sampling rate, the amount of processed data is also less, which can be a benefit for the real-time control of a myoelectric prosthesis.

The eight sensors were enclosed in the same silicon band used in setup 1, as shown in Figure

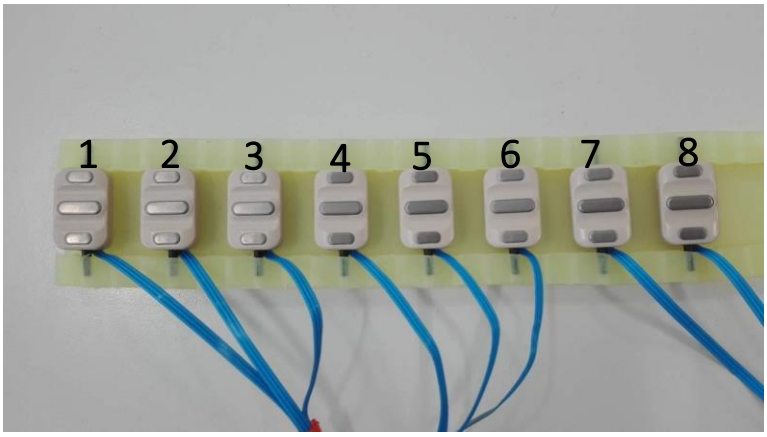

Figure 3.2: The OttoBock sensors enclosed in the silicon band according to setup 2. The numbers given to the sensors match the ones given to the ones from the Myo Armband in setup 2

3.2, around 1 cm away from each other. A number was given to each of the sensors, from 1 to 8, that match the ones given to Myo system in setup 2, similarly to setup 1 of both systems.

3.2 THE MYO SYSTEM

"Myo System" was the name given to the Myo Armbrace, a commercially available low-cost device which can be used on the forearm to control video-games, music and visual entertainment. This device features eight sEMG sensors, an accelerometer, a gyroscope, a magnetometer (inertial sensors) and a Bluetooth connection for data transfer. The sEMG signals are acquired at a frequency of 200 Hz with an 8-bit resolution. It is important to point out that the sEMG signal acquired is "raw", that is, it lacks any filtration and it is not enveloped. For information, the data from the inertial sensors is sampled

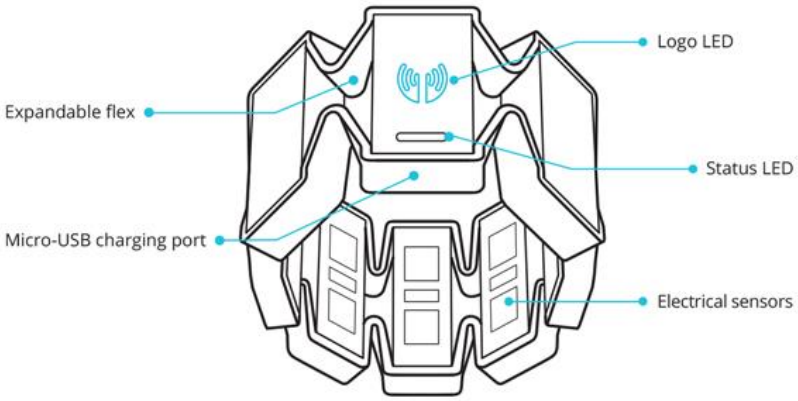

Figure 3.3: The main components of the Myo armband, which can be used as reference points [54]

at 50 Hz, also with an 8-bit resolution. Although the inertial sensors can have an important role to play in several applications, they were not used on the course of this work because the point is to compare

the sEMG sensors from both systems. Figure 3.3 illustrates some of the reference points of the Myo Armband.

The Myo Armband has the advantage of having an affordable price and being easy to use. It can be bought online, on its official website [14], for the price of $199. Considering the OttoBock sensors have a price of around $400 each (total cost equal to $3,200, without considering the elastic band and the data acquisition and transmission components that are integrated in Myo System), the cost difference between the Myo System and the OttoBock system is quite considerable.

Because the number of sensors used on the two experiments was different, two different setups were also considered for the Myo system.

3.2.1 Setup 1 and 2 correspondences for the Myo System

For the Myo system, conversely of the OttoBock system, no hardware changes were necessary, only the number of sensors used differ from one setup to another. In setup 1, only five out of the eight sensors were used, as depicted in Figure 3.4(a). On the other hand, in setup 2, all the available sensors were used, as it can be observed in Figure 3.4(b). The selected sensors from each setup were numbered correspondingly in order to match the respective sensors from the OttoBock system.

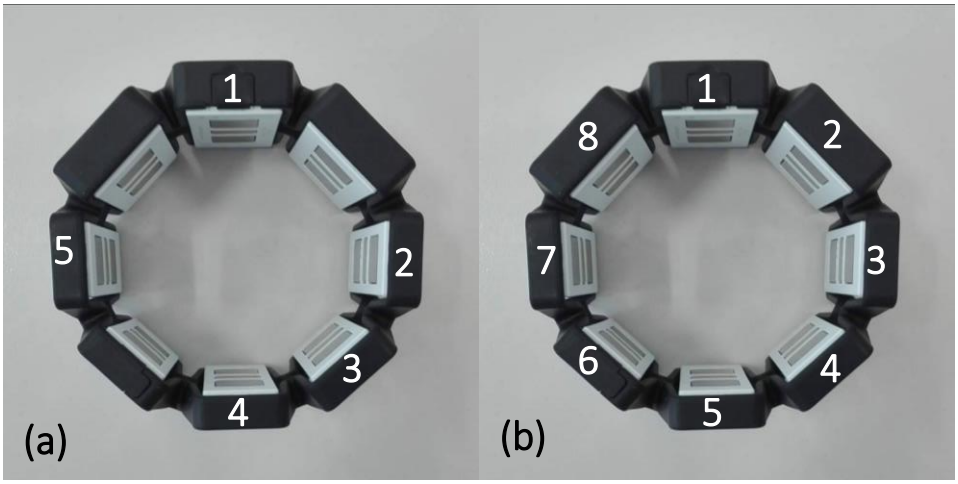

Figure 3.4: The setup 1 and order given to the sensors (a). Setup 2 and respective numbers for each sensor (b). For reference, the micro-USB charging port is in sensor 1 and it is pointing upwards.

3.3 SOFTWARE

For the OttoBock system, the *firmware* was written and loaded to the Arduino using Arduino IDE [55] and data was acquired using MATLAB. For the Myo System, a downloadable software from the official site called "*Myo Data Capture*" [56] was interfaced with MATLAB for recording data. All signal processing and data preparation for classification were also performed using MATLAB. All the classifications were done using Weka [57], a free software developed at the University of Waikato, New Zealand, that features a large collection of machine learning algorithms for data mining tasks. Finally,

all the statistical tests were performed using R [58], a free software environment for statistical computing and graphics.

4 EXPERIMENT 1: GESTURE RECOGNITION VALIDATION

The objective of this first experiment was to try out different combinations of signal processing techniques and pattern recognition algorithms, and to evaluate which of them could be the best solution for the recognition of four different hand gestures. The hypothesis that the data acquired using the Myo System could generate classification results as good as, or better than, the OttoBock System could be validated with a positive outcome of this experiment. This would mean the project could advance for sEMG measurements on transradial amputees. It was crucial to validate such hypothesis before moving on in order to further validate gesture recognition on amputated patients and to ensure that both systems were working conveniently.

4.1 METHODS

In this experiment, both Myo and OttoBock systems are used, configured as described in chapter 3 – setup 1. In order to base the work on comparable data, and due to an initial limitation on the availability of the OttoBock sensors, for this particular experiment the observations were done using a number of five sensors, placed exactly in the same positions, for each of the systems. As previously mentioned, the data was sampled at 1 KHz for the OttoBock system and at 200 Hz for the Myo system.

The target of the experiment is the recognition of four hand gestures, depicted in Figure 4.1 and described below. In the following, the term "loop" refers to a complete set of these four gestures, in the presented order:

1. **Rest**: hand relaxed on the table, with the palm facing down.
2. **Grasp**: hand with all fingers closed while the elbow is on the table. Approximately, 45˚ in the angle between the forearm and the table.
3. **Extension**: hand opened and stretched while the elbow is on the table. Approximately, 45˚ in the angle between the forearm and the table.
4. **Pinch**: hand with thumb and finger touching as in the gesture of picking a small object, while the elbow is on the table. Approximately, 45˚ in the angle between the forearm and the table.

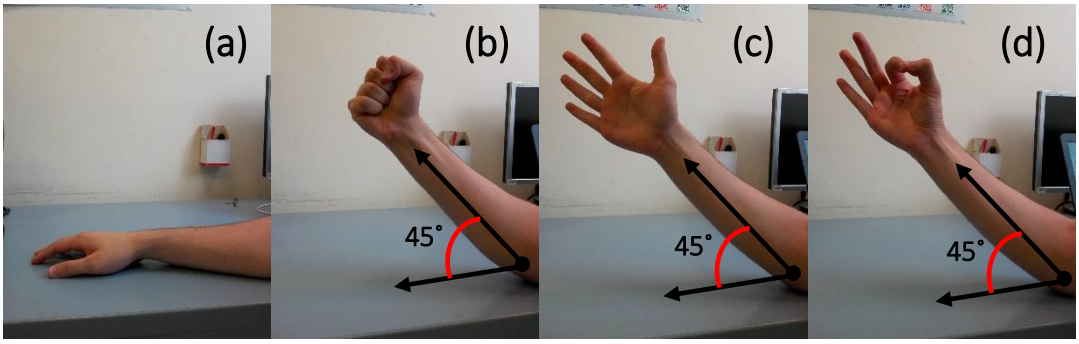

Figure 4.1: The 4 hand gestures: Gesture 1 - Rest (a); Gesture 2 - Grasp (b); Gesture 3 - Extension (c); Gesture 4 - Pinch (d)

In total, nine subjects participated in the task: seven of them were male and two were female. All of them were healthy, without any muscular or neurological diseases; the average age of the participants was 29.4 with a standard deviation of ± 9.8 years.

The experiment consisted on the visualization of a simple video where a picture of each gesture was shown for 10 seconds in the same order referred above, for 10 loops. The subject was supposed to imitate the gestures as they were shown in the video with his right hand. Therefore, each gesture was repeated 10 times and recorded for 10 seconds. This procedure was done separately for each system. To evaluate repeatability and reproducibility, the experiment was divided into two sessions, on two separate days, for every subject. The used protocol for both sessions was the same.

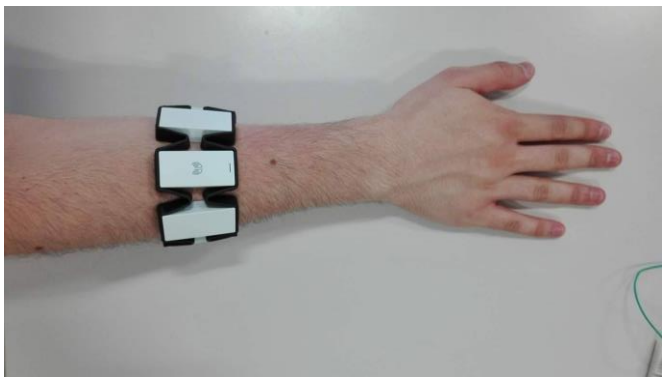

Figure 4.2: How the Myo Armband was placed on the forearm

In each session, the first system used was the Myo. The system was wrapped around the subject's right forearm, in the mid-point between the wrist and the elbow, as depicted in Figure 4.2. Sensor 1 was placed above the *extensor carpi ulnaris*, with the micro-USB charging port pointing in the distal direction. Due to the particular Myo elastic band support, the remaining eight sensors assumed an equal distance apart from each other. Having this in consideration, one could state with sufficient approximation that the sensors 2,3 and 4 were above *flexor digitorum superficialis* and *brachioradialis* while sensor 5 was above *flexor carpi ulnaris*. Based on an empirical point-of-view, with respect to the selected hand gestures, from the possible configurations between the eight Myo sensors, the one described in setup 1 allowed the best differentiation between the sEMG patterns.

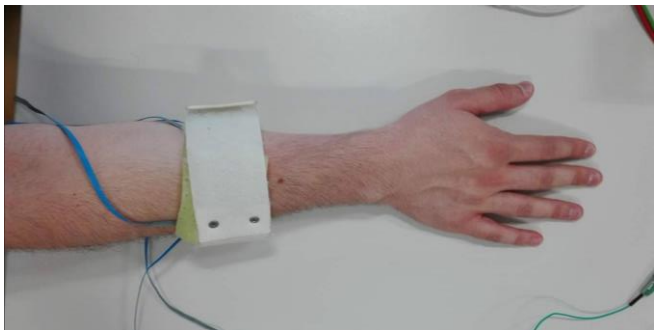

Figure 4.3: A Velcro strap was wrapped around the silicon bracelet, to make sure the OttoBock system was tight around the forearm

The positions of the Myo sensors were marked with a pen on the subject's skin before switching the Myo system with the OttoBock. After the Myo armband was removed from the subject, the OttoBock system was wrapped around the subject's forearm, and with the help of the markers, the OttoBock sensors were carefully placed in the same position of the sensors of the Myo system, respecting also the orientation and the numbering. A white Velcro strap was used to make the system tight around the subject's forearm, as visible in Figure 4.3.

The protocol used for each session of this experiment is presented below:

1. First, the subject is asked to sit comfortably in a chair in front of a table and a screen;
2. The experiment's protocol is explained briefly to the subject;

3. The Myo system is wrapped around the subject's right forearm, as described before;
4. The subject is asked to put the right hand on the table, in the rest position, and wait until the video starts;
5. The sEMG recording starts;
6. The video is played on the screen;
7. The subject is supposed to replicate each gesture for as long as it is shown in the screen (10 seconds per gesture). Each gesture is replicated 10 times, in the order referred above;
8. The video reaches its end, the subject gets back to the rest position and waits;
9. The recording is stopped, and the subject is told that he can move his arm freely;
10. The position of the five selected sensors from Myo system are marked in the subject's arm, using a pen;
11. The Myo system is taken off from the subject's forearm;
12. The OttoBock sensors are placed exactly in the same location where the five Myo Armband sensors were (the OttoBock sensors position can and should be adjusted in the silicon band for each different subject);
13. The subject is asked again to put his arm in the rest position and wait;
14. The steps 4 to 9 are repeated;
15. The OttoBock system is removed from the forearm and the session is finished.

After the sEMG data from both the sessions of all the nine subjects was collected, it was processed and analysed using MATLAB. The data recorded for each subject before the first loop and after the last was deleted and all the meaningful data was stored in a $[L \times S]$ matrix, where $L = 1000000$ (10 seconds of recording for each gesture, 10 repetitions of the same gesture, 1KHz sampling frequency) for the OttoBock system and $L = 20000$ (10 seconds of recording for each gesture, 10 repetitions of the same gesture, 200 Hz sampling frequency) for the Myo system. Since the number of sensors used was five: $S = 5$ for both systems. These values reflect well the high amount of data that is being processed in this situation.

4.1.1 Frequency Analysis

Before moving on to signal processing, it was essential to acquire more information about the acquired signal. A factor that could be important was the information about the signal's frequency. This information could be relevant to decide the cut-off frequency for filtering and to understand the downsampling amount parameters, in order to reduce the quantity of data for classification. To convert the acquired signal from its time domain to the frequency domain representation, the FFT (Fast Fourier Transform) algorithm was used. This algorithm computes the discrete Fourier transform of a sequence.

For the frequency analysis, the full signal with a total duration of 400 seconds (10 repetitions of 10 seconds recording for each of the 4 gestures) was discretized into 1 second segments, for each sensor channel. The FFT was applied to each of the 1 second segments. Afterwards, the results from the FFT of all 400 segments were averaged for each sensor. The average of all the sensors was calculated for each subject. The FFT results from all subjects were also averaged for each session and for both systems. Results are shown in Figure 4.4 and Figure 4.5, for OttoBock and Myo systems, respectively. Because the signal from the OttoBock is already enveloped, as referred before, the signal from the Myo system was also enveloped using the Hilbert transform before the application of the FFT algorithm. This way, it is possible to have a more reliable comparison between the power spectra from both systems.

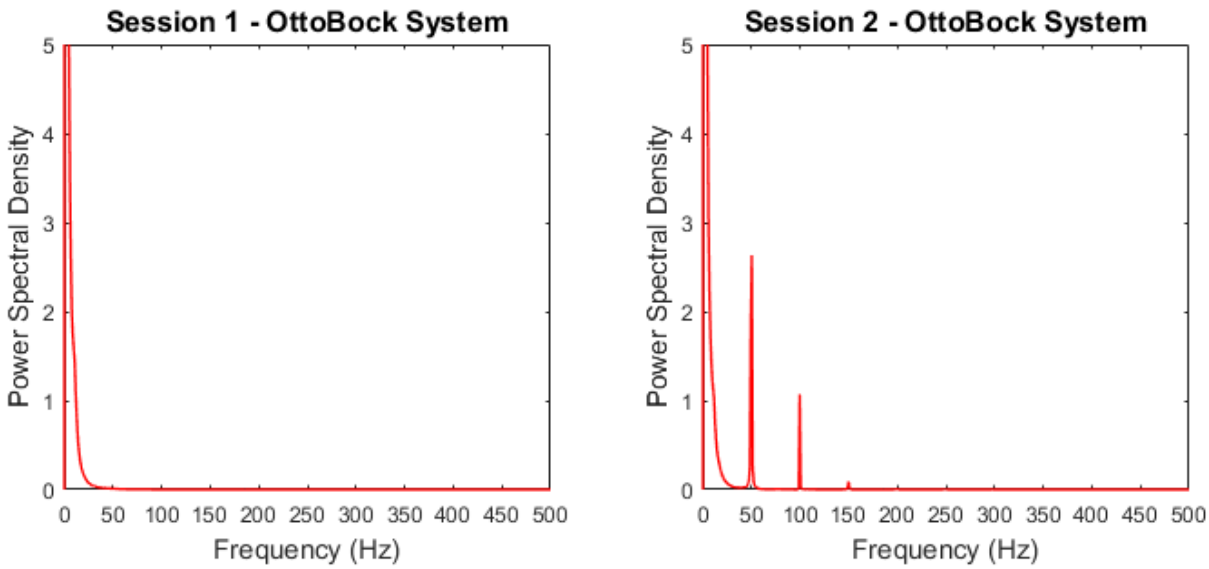

Figure 4.4: Power spectra from session 1 (on the left) and session 2 (on the right) extracted from the sEMG signal acquired using the OttoBock system

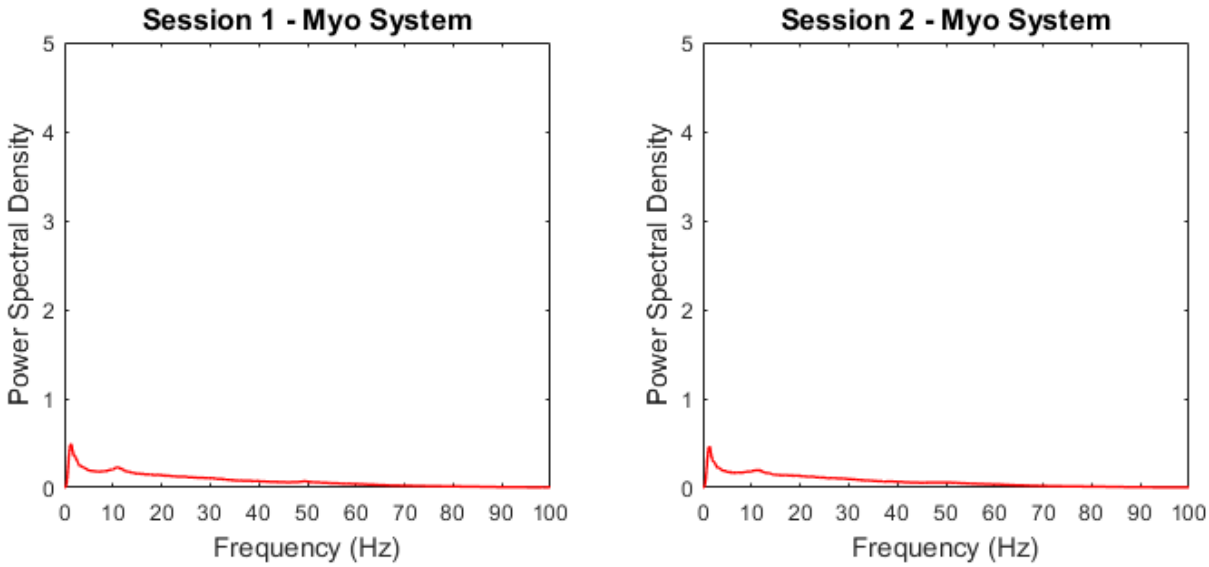

Figure 4.5: Power spectra from session 1 (on the left) and session 2 (on the right) extracted from the sEMG signal acquired using the Myo system

On Figure 4.4, for both sessions, it can be observed that as the frequency approaches 0 Hz the power spectral density increases abruptly, which means the most relevant frequencies from the signal have a very low frequency. However, in the power spectrum from the session 2 there is a peak in 50 Hz, a smaller one in 100 Hz and another one at 150 Hz. This means that these frequencies could be filtered because they are not important for the signal and represent noise that comes from the electrical network.

In the power spectra extracted from the Myo signal (Figure 4.5) it can also be observed the increase in power spectral density as the frequency approaches 0 Hz. However, it can be observed that the values of power spectral density are not so high as in the OttoBock's case and there is a peak near the 1 Hz mark. Much like the previous scenario, it is also observable that the power spectral density seems to stabilize near zero after the 50 Hz mark.

Overall, there are two important conclusions that can be taken from this frequency analysis:

- The most relevant frequencies for the sEMG signal seem to be less than, approximately, 50Hz. This is verified in the signals acquired from both systems. As referred in section 3.1.1, the Nyquist Theorem states that sampling frequency from a signal should be more than twice its frequency. This means that it could be possible to artificially reduce the sampling frequency from both systems to 100 Hz.
- Very low frequencies seem to have an important role in the signals acquired, so a low frequency like 1 Hz can be a good cut-off frequency to use in a low-pass filter and remove the unwanted noise from the signal. 1 Hz might seem a very low value to use as cut-off frequency because it might result in loss of information related with fast variations of the signal. However, for classification purposes, only the steady-state signal is used from each gesture acquisition, which means that it is not necessary to use a wide band.

4.1.2 Signal Processing and Feature Extraction

Regarding signal processing, several approaches were made to evaluate which ones could generate the better classification outcome. Each of these approaches was called a "setting". Each of the settings chosen is described below:

- **Setting 1**: No signal processing was applied to signals from both systems, so the signals were kept "raw", just as they were acquired. It can be interesting to observe how the classifiers behave with a signal that holds no digital processing;
- **Setting 2**: Because the signal from the OttoBock sensors comes already enveloped, an envelope (using absolute value and the Hilbert transformation functions from MATLAB) was applied to the signals from the Myo sensors for a better comparison. A low-pass Chebyshev filter was also applied to both signals with a cut-off frequency of 1 Hz. By reducing the signal's noise, the classification performance might improve due to less chance of overfitting (described in section 2.3.5.2);
- **Setting 3**: Data acquired from both sensors was downsampled to 100 Hz and were previously filtered by a Chebyshev low-pass filter with a cut-off frequency of 45 Hz to avoid aliasing. As observed in the frequency analysis, this sampling frequency can be used without losing too much information from the signal. This can be helpful to reduce the amount of data given as input to the classifier and reduce the classification time, which, in a real-time application is crucial. The signals from the Myo sensors were previously enveloped.
- **Setting 4**: Same as setting 3, but filtered with a low-pass Chebyshev filter, using a 1 Hz cut-off frequency, instead of 45 Hz. The point was to eliminate as much noise as possible to the downsampled signal;
- **Settings 5 and 6**: (Described below).

Since the recording was continuous, when the subject changes hand gesture, there is a huge peak in the sEMG signal from some sensor channels of both systems, as it can be observed in Figure 4.6 and Figure 4.7. This can be due to the movement of the electrodes on the patient's skin, which can cause values to oscillate very quickly. However, steady-state sEMG signal are more robust than transient signal for classification purposes [31]. Considering this, the first 4 seconds from the 10 seconds of each gesture acquisition were erased and only the last 6 seconds of steady-state signal were used for classification.

Each of the 4 gestures was acquired 10 times, leaving us with 40 instances to classify. To perform meaningful classification, it is important to have a higher number of instances to classify. Therefore, each of the final 6 seconds from each gesture acquisition was divided into 10 segments of 600 ms. Therefore, a 600 ms window length was used. This leaves us with 400 instances to classify, 100 for each gesture, which can allow richer results. This method was applied for every setting.

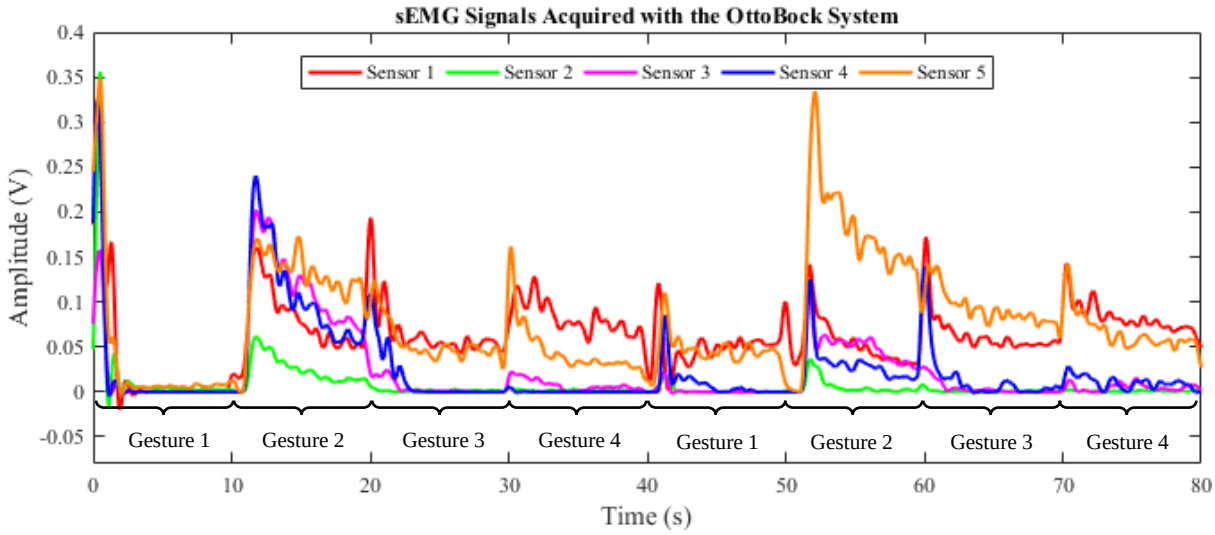

Figure 4.6: First two loops recorded with the OttoBock system. The data belongs to the first session of subject 2 and setting 2 is being used.

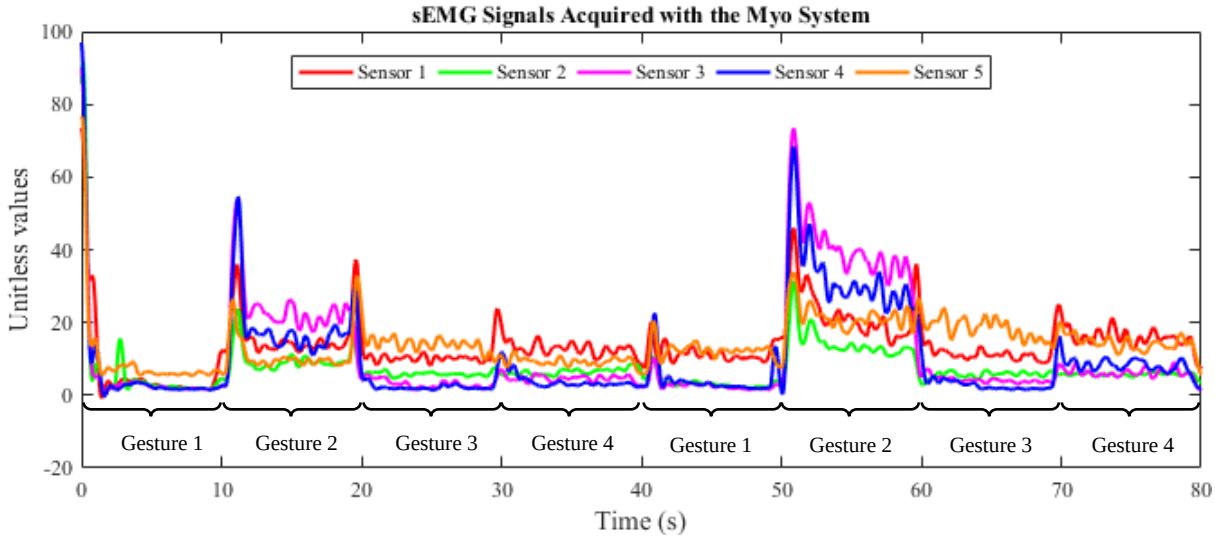

Figure 4.7: First two loops recorded with the Myo system. The data belongs to the first session of subject 2 and setting 2 is being used. Since the sensors are part of a commercial product, there is no information about the voltage output. The data acquired is given in unitless integers.

The 400 instances obtained from each setting, containing all the values from each sensor, were given directly as input to the classifiers, without any feature extraction.

Some patterns can be very similar in the time domain but can become more distinguishable when projected in the frequency domain. Therefore, the only feature extraction performed was the power spectrum by applying the FFT algorithm on each of the 400 segments from setting 1 and 2. These new two combinations were given the name, respectively, of **setting 5** and **setting 6**.

4.1.3 Classification

For the classification process, six pattern recognition algorithms (which are thoroughly described throughout section 2.3) were selected:

1. **LDA**: Linear Discriminant Analysis;
2. **Linear SVM**: Support Vector Machine with no usage of Kernels;
3. **Polynomial SVM**: Support Vector Machine with polynomial Kernel;
4. **SMO**: Support Vector Machine with polynomial Kernel and Sequential Minimum Optimization for the solving of the QP optimization problem;
5. **Naïve Bayes**: learning algorithm that uses the Bayes rule;
6. **kNN**: *k* Nearest Neighbours, with $k = 1$.

The choice of these classifiers was based on their relative simplicity and easy implementation. Due to these characteristics, it is expected to have a fast classification process, which is essential for real-time systems, like myoelectric prothesis. Besides, in other works, all of them have been already implemented with success to gesture recognition tasks, as commented in section 2.3.

To evaluate classification accuracy, the data relative to session 1 was classified using a 10-fold cross validation method, iterated 10 times. On the other hand, for session 2, the classification accuracy was evaluated using the train-test method with three different combinations of training and testing sets, which were given the name of "Train-Test sets":

- **Train-Test set 1**: Training set: Session 1 data set; Testing set: Session 2 data set;
- **Train-Test set 2**: Training set: Session 1 data set, plus 25% of the session 2 data set; Testing set: Remaining 75% from session 2 data set;
- **Train-Test set 3**: Training set: 25% of the session 2 data set; Testing set: Remaining 75% from the session 2 data set.

Overall, 6 different combinations of signal processing techniques and features extraction were used for classification, using 6 pattern recognition algorithms. This generated a large set of results for both sEMG systems and some interesting conclusions.

4.2 RESULTS

In this sub-chapter, all the classification results obtained from the sEMG data acquired in experiment 1 are presented. To all statistical tests, a 5% significance level was used. Also, all the presented results are discussed according to accuracy, which is defined in section 2.3.6.

4.2.1 10-Fold Cross-Validation Evaluation

This section will start by examining the results from the session 1 data set, where the 10-fold cross-validation was applied. First, the classifiers accuracies obtained using the Myo system will be examined, followed by the OttoBock system.

4.2.1.1 Myo System Results

In Figure 4.8, it is possible to observe the accuracies obtained for the Myo system by each of the used classifiers, organized by setting. The poorer results were found for setting 1, where no signal processing was applied to the sEMG signal. In this case, all classifiers performed poorly (below the 50% mark), except for the Bayes classifier, which managed to obtain an 82.38±5.57% accuracy. However, in setting 2, with enveloped and filtered signal, the results were very much different, achieving a maximum accuracy of 95.72±2.93% with kNN. A non-parametric Friedman test with post hoc [59] was applied to the accuracies obtained for this setting and Polynomial SVM, SMO and kNN were found to be the classifiers with better results, with no significant differences between them.

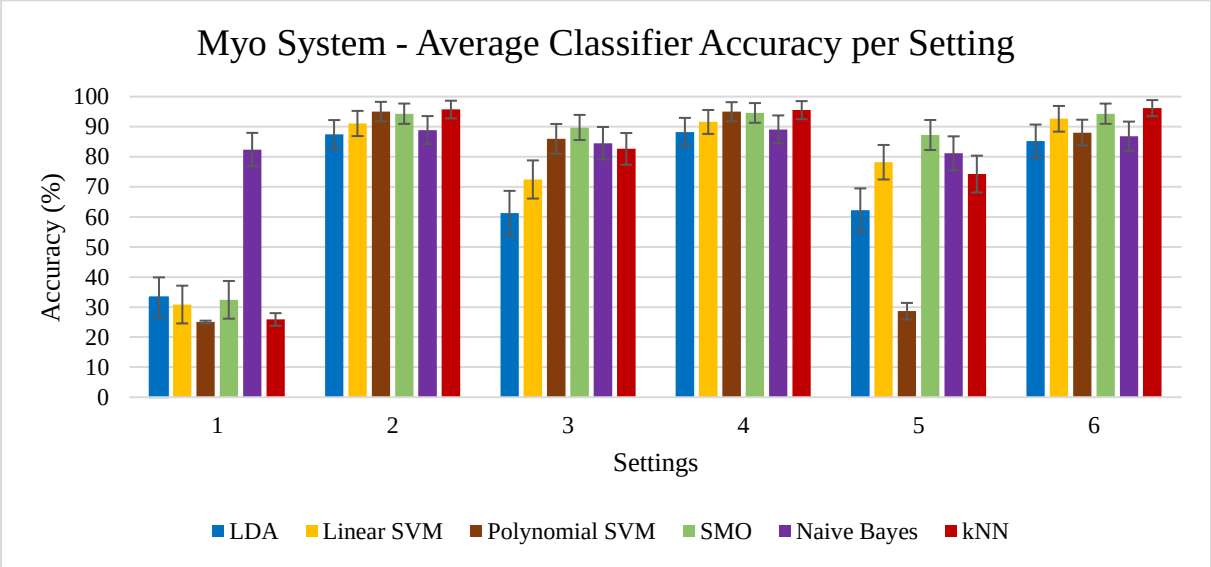

Figure 4.8: Average classifier accuracies per setting, using the Myo System and cross-validation evaluation

From observing the bar plot, it is interesting to observe that the results from setting 2 are very similar to setting 4, with kNN achieving also the maximum accuracy among all the classifiers (95.5±93.01%). Both are low-passed filtered at 1Hz, but in setting 4 the signal was downsampled to 100Hz, unlike setting 2, where the sampling frequency was left unaltered at 200Hz. The results from a Friedman test with post-hoc for setting 4 also concluded the best classifiers to be Polynomial SVM, SMO and kNN with no significant differences between them. A paired t-test was also applied to each pair of Polynomial SVM (p-value = 0.842), SMO (p-value = 0.646) and kNN (p-value = 0.842) classifiers from both these settings. No significant differences were found.

Table 4.1: Average accuracy of all classifiers for Myo System, using cross validation

Average Accuracy of all Classifiers for Myo System		
Setting	Accuracy (%)	S.D.
1	38.30	5.13
2	92.07	3.93
3	79.43	5.68
4	92.33	3.86
5	68.60	5.60
6	90.54	4.26

Accuracies from setting 3 were lower than settings 2, 4 and 6, which is more evident by observing the average accuracy of all classifiers per setting, shown in Table 4.1. However, it still calculated an 89.75±4.18% accuracy with the usage of SMO.

Finally, let us observe the results from the FFT feature extraction: settings 5 and 6. Although the accuracies obtained using setting 5 were lower than expected, setting 6 produced high accuracies and obtained the maximum classification accuracy between all the settings, 96.18±2.68%, using kNN. A Friedman test with post hoc concluded that the best classifiers for setting 6 were the SMO and kNN, with no significant differences between each other.

The optimal accuracy for the Myo system was the one calculated using kNN on setting 6, since it was the overall maximum.

4.2.1.2 OttoBock System Results

As presented for the Myo system, in Figure 4.9, the accuracies obtained for the OttoBock system by each of the classifiers, organized by setting, can be observed. At first glance, all the settings were capable to produce positive results, even without any signal processing, as it can be confirmed by the average accuracy of all classifiers per setting shown in Table 4.2.

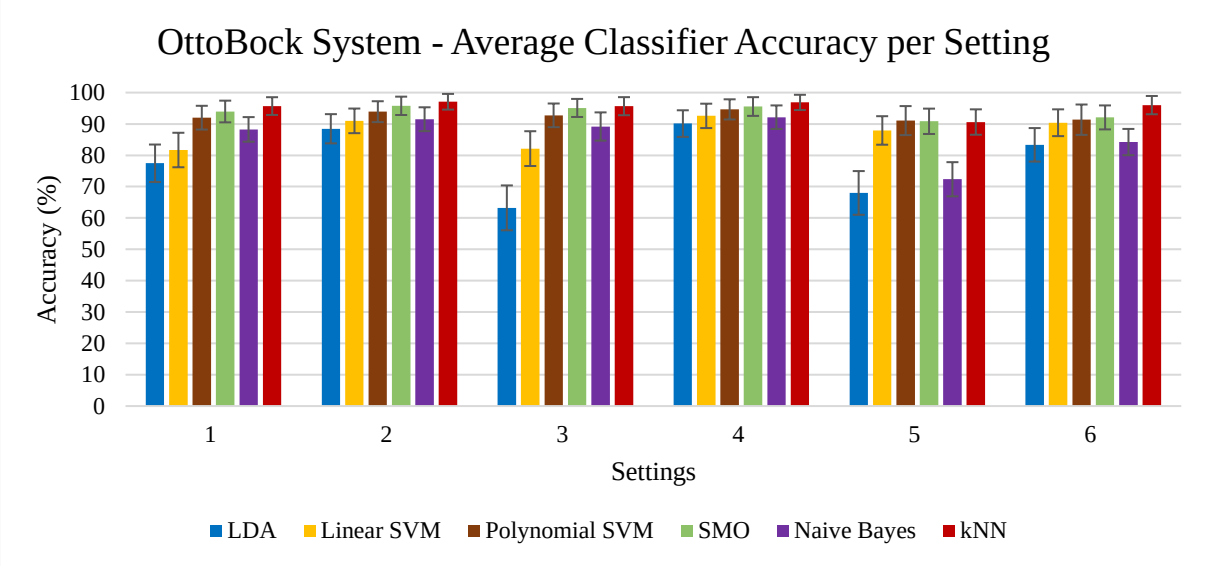

Figure 4.9: Average classifier accuracies per setting, using the OttoBock System and cross-validation evaluation

The classifier that calculated the best accuracy in most settings was the kNN. A maximum accuracy of 97.08±2.50% for the OttoBock system was obtained using the very same classifier on setting 2. Due to the high values of general accuracies, a Friedman test with post hoc was applied to each of the settings to understand which were the best classifier(s) in each case, with no significant differences between them. The results are shown in Table 4.3.

As it can be observed, in most of the settings, accuracies from SMO and kNN have significant differences from the ones calculated with other classifiers, but not between each other. However, in most of the cases, kNN always provides a higher accuracy than SMO. Overall, the best classification was by kNN in setting 2, since it was the overall maximum.

As a side note, it is also interesting to observe that, much as the results from Myo system, the accuracies from setting 2 and 4 are very similar. This can be seen in Figure 4.9 and Table 4.2.

Table 4.2: Average accuracy of all classifiers for OttoBock System, using cross validation. "SD" stands for Standard Deviation

Average Accuracy of all Classifiers using OttoBock System		
Setting	**Accuracy (%)**	**SD**
1	88.18	4.39
2	92.95	3.59
3	86.34	4.71
4	93.65	3.47
5	83.46	5.05
6	89.56	4.30

Table 4.3: The best classifiers for each setting, with no significant differences between them

Setting	**Best Classifiers**
1	SMO, kNN
2	SMO, kNN
3	SMO, kNN
4	kNN
5	Polynomial SVM, SMO, kNN
6	kNN

4.2.2 Train-Test Evaluation

In this next section, the results from train-test evaluation will be discussed, applied as described in section 4.1.3, for both systems. For each system three different combinations of training and testing sets were used. Each of these combinations was called "train-test set" and all of them will be discussed. As before, the results from the Myo system will be discussed first, followed by the OttoBock system.

4.2.2.1 Myo System Results

The classifier accuracies of each setting are represented in the bar plots from Figure 4.11, 4.12 and 4.13, for train-test sets 1, 2 and 3, respectively. It is noticeable that there are some differences between the accuracies from each train-test set. The differences in accuracy are more noticeable by observing Figure 4.10, where the total classifier averages from the six settings are represented for each train-test set. A large difference can be observed between train-test sets 1 and 2 and a smaller one between train-test sets 2 and 3, which means that adding data from session 2 to the training set substantially increases classification performance. It also appears that removing the data from session 1 from the training set and just using data from session 2 is better than using both. Because train-test set 3 produced the best results, it deserves to have a deeper analysis.

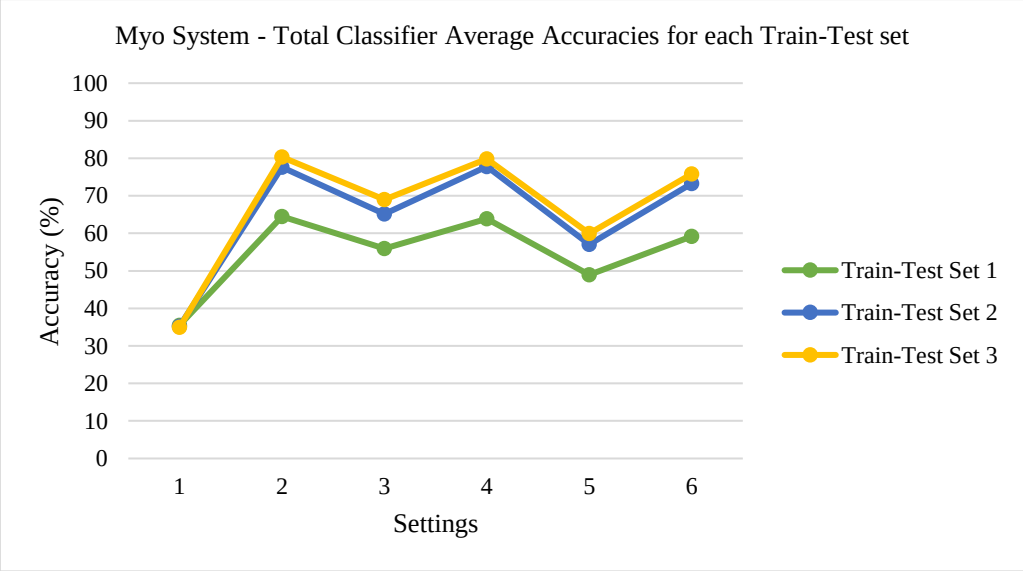

Figure 4.10: Total Classifier Average Accuracies for each Train-Test set, using Myo system

As observed in the cross-validation evaluation for the session 1 data set, results from setting 1 are very weak. The higher accuracies are present again in settings 2, 3, 4. As before, a Friedman test with post hoc was performed for each of these three settings. SMO was found to be the best classifier for all the three settings, with significant differences from all the other classifiers.

As observed in previous results, the accuracies from setting 2 and 4 are very similar, even if the sampling frequency used in setting 4 (100 Hz) is half of the one used in setting 2 (200 Hz). To confirm that the same kind of results can be obtained using both settings, a paired t-test was performed to compare the results from SMO, the best performing classifier, in both these settings. The results indicated that there was no significant difference between the classifier in both settings (p-value = 0.077).

The maximum accuracy (88.07±6.87%) was calculated in setting 2, using the SMO classifier. Because of this, it was considered to be the optimal accuracy obtained for this system, while using the train-test evaluation method.

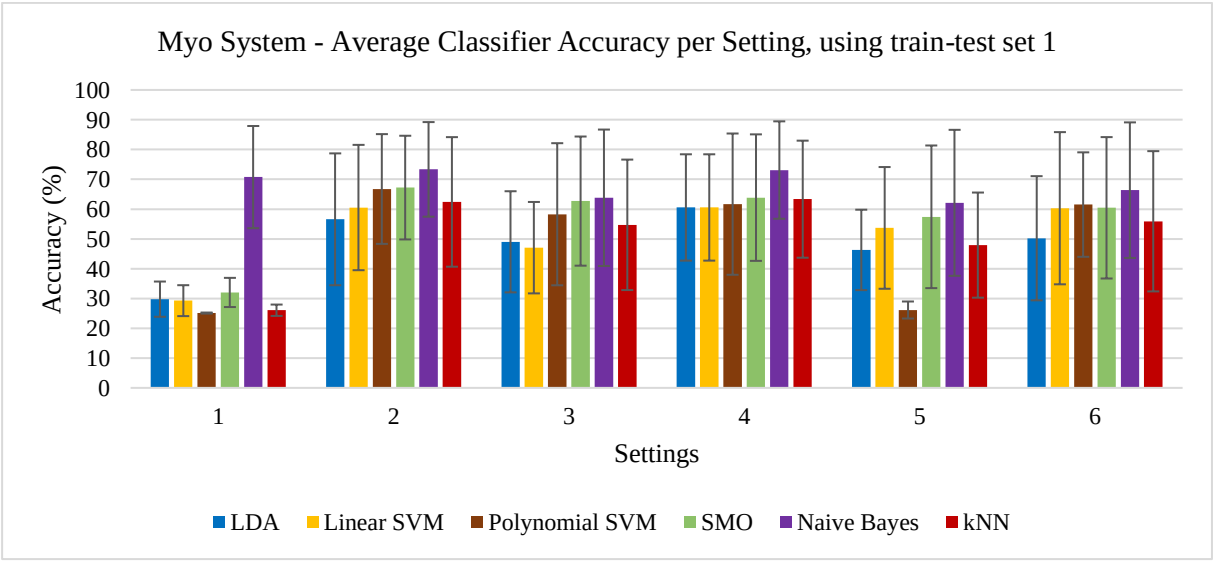

Figure 4.11: Average classifier accuracies per setting, using the Myo system and train-test evaluation (according to train-test set 1)

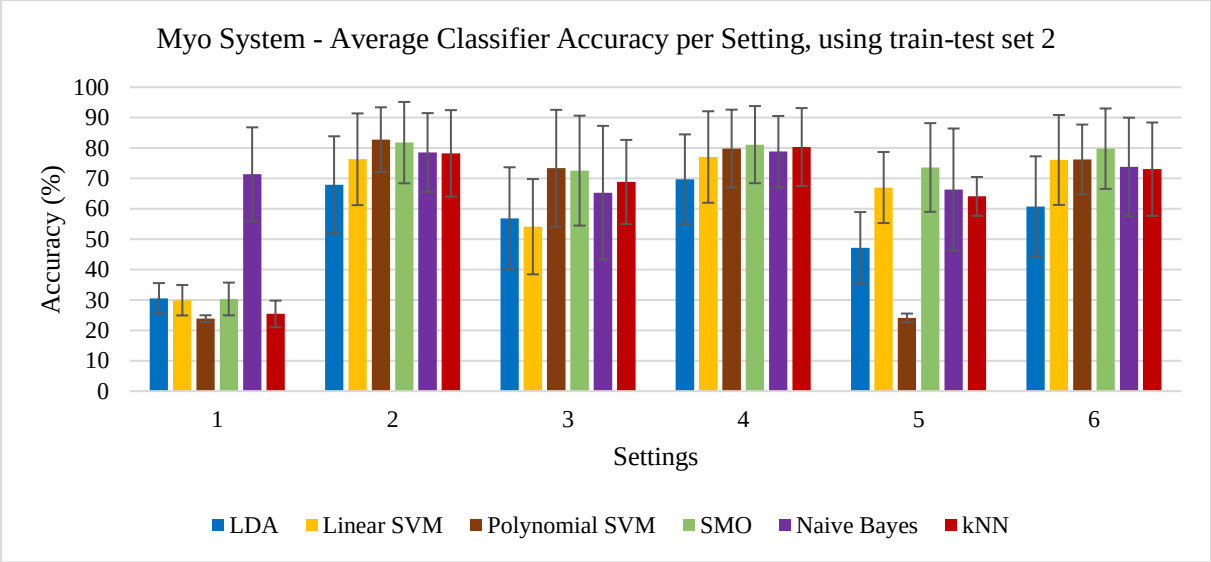

Figure 4.12: Average classifier accuracies per setting, using the Myo system and train-test evaluation (according to train-test set 2)

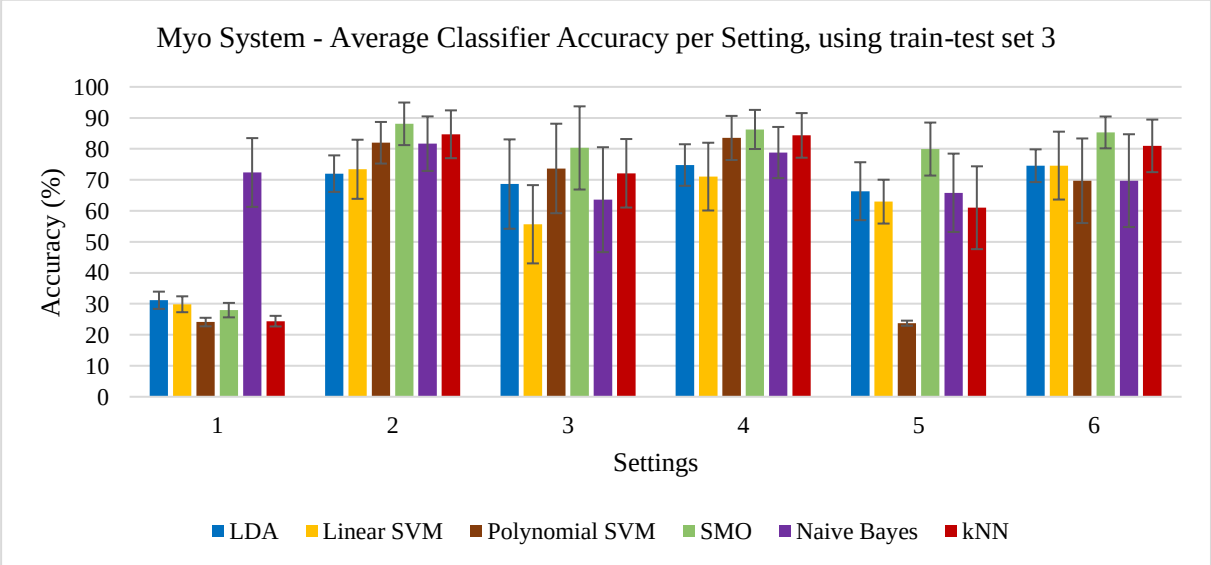

Figure 4.13: Average classifier accuracies per setting, using the Myo system and train-test evaluation (according to train-test set 3)

4.2.2.2 OttoBock System Results

Much like the results from the Myo systems, the accuracies obtained with the train-test set 3 (Figure 4.17) were superior to the ones from train-test sets 1 and 2 (Figure 4.15 and Figure 4.16, respectively). As in the Myo system's case, the average accuracies from each setting were compared between train-test sets in Figure 4.14. The scenario is quite close to the previous one, there is a big improvement between the accuracies from train-test sets 1 and 2 and a smaller one from train-test set 2

to 3. However, the improvement from train-test 2 to 3 is visibly higher than in the Myo system. Because of the higher results, train-test set 3 will be subjected to further analysis.

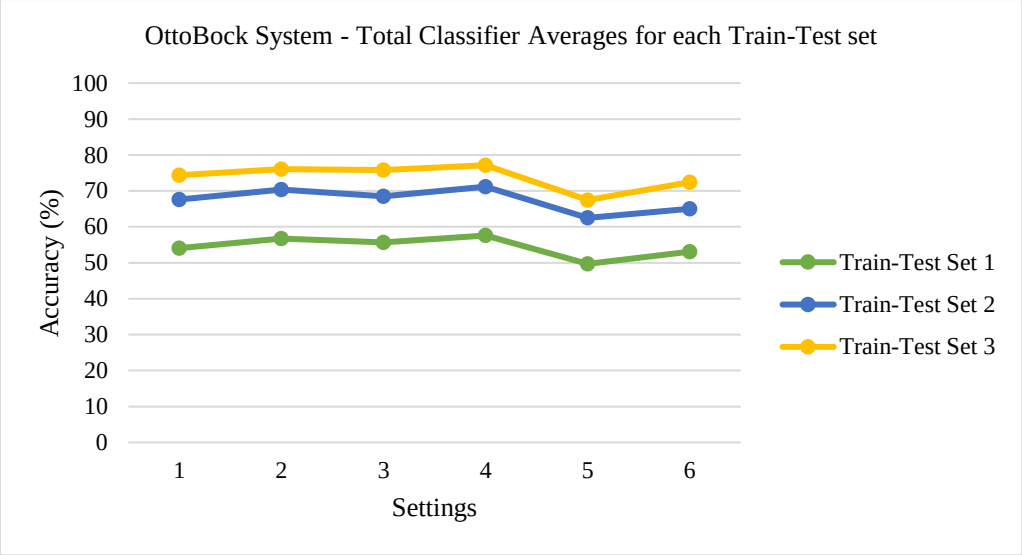

Figure 4.14: Total Classifier Average Accuracies for each Train-Test set, using OttoBock system

Like the OttoBock system's situation when using the cross-validation method on session 1 data set, the accuracies between settings are very similar. However, Polynomial SVM and SMO seem to produce the best results, in a general way. To verify if there are any significant differences between classifiers for each setting, a Friedman test with post hoc was executed. In Table 4.4 the best classifiers are represented for each setting, with no significant differences between them.

Table 4.4: The best classifiers for each setting, with no significant differences between them

Setting	Best Classifiers
1	Polynomial SVM, SMO, Naïve Bayes, kNN
2	Polynomial SVM, SMO, Naïve Bayes, kNN
3	Polynomial SVM, SMO, Naïve Bayes, kNN
4	Polynomial SVM, SMO, Naïve Bayes, kNN
5	Linear SVM, Polynomial SVM, SMO, kNN
6	Polynomial SVM, SMO, kNN

Although Polynomial SVM, SMO and kNN have significant differences from the other remaining classifiers, Polynomial SVM seems to produce the higher accuracies for each setting (except for setting 6, where SMO outperforms). This classifier even provides the highest calculated accuracy, 81.85±9.56%, in setting 4. This was considered to be the optimal accuracy for this system.

It is interesting to observe that the accuracies from setting 1, where no signal processing was applied, had an almost equal performance to settings 2, 3 and 4 where filtering and/or downsampling techniques were applied. This means that the sensors provide a high-quality signal, ready to be used for classification purposes if the user desires to do so.

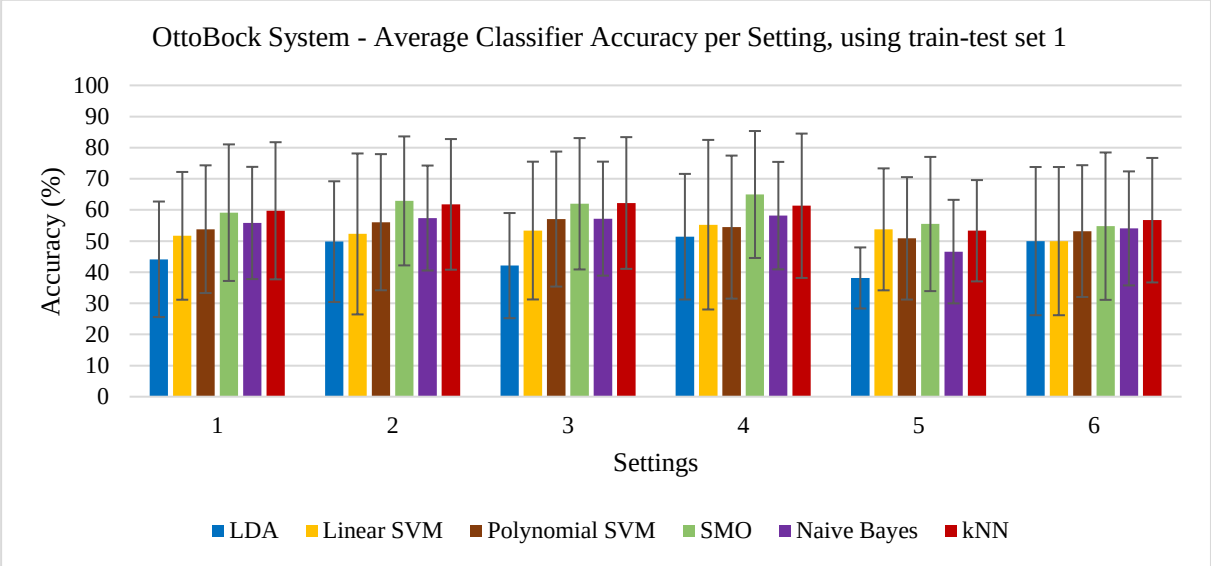

Figure 4.15: Average classifier accuracies per setting, using the OttoBock system and train-test evaluation (according to train-test set 1)

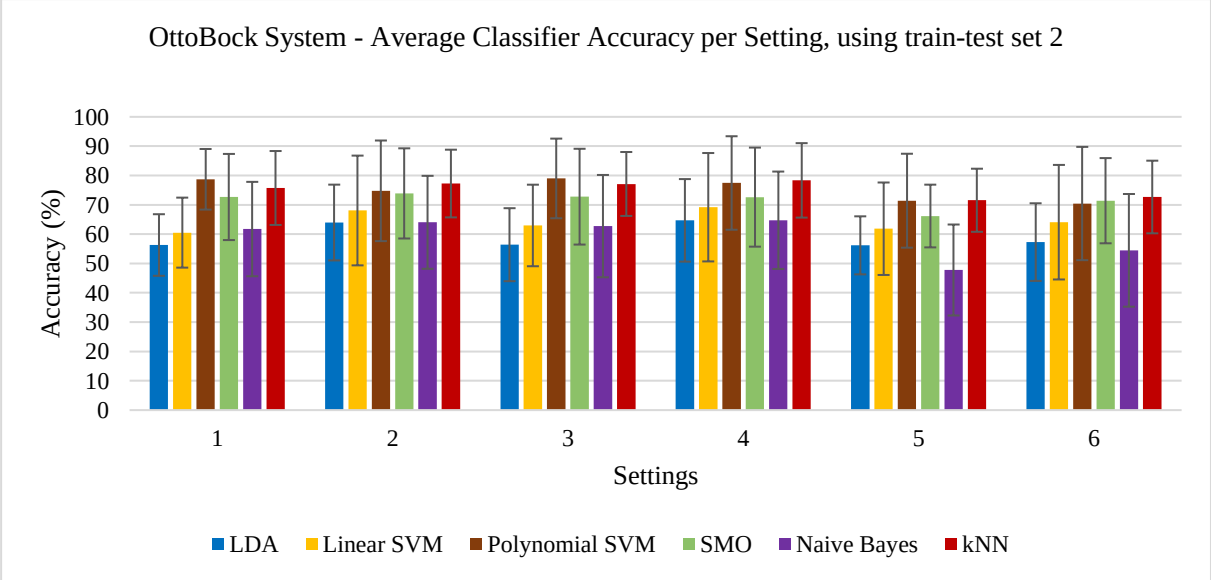

Figure 4.16: Average classifier accuracies per setting, using the OttoBock system and train-test evaluation (according to train-test set 2)

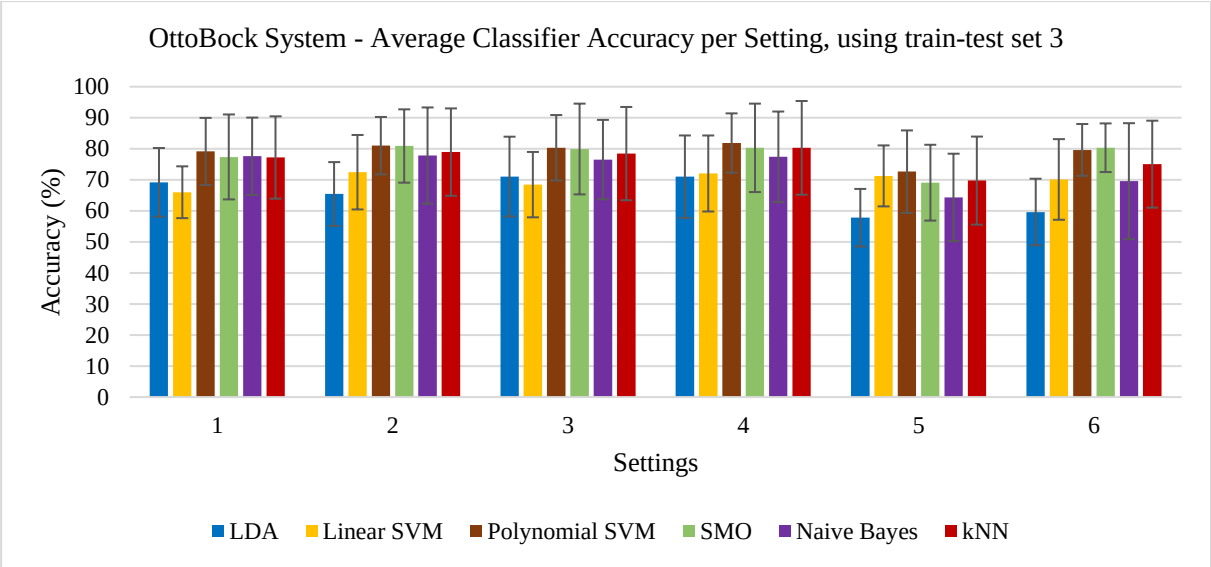

Figure 4.17: Average classifier accuracies per setting, using the OttoBock system and train-test evaluation (according to train-test set 3)

4.2.3 Training and Testing time analysis

When using classifiers in real-time applications, such as the control of a myoelectric prosthesis, it is paramount to take into account how much time the chosen classifier takes for training and testing. When calibrating a myoelectric prosthesis that uses gesture recognition algorithms, it is necessary for the user to perform a certain set of gestures, to train the classifier. It is therefore important that the time for training is reduced, so that the user does not have to wait too much time before using the equipment. However, the time that the classifier takes to classify each gesture, or instance, is of greater relevance in real-time application. This time interval plays an important role on determining how long it takes for the actuators to be activated after the user performs the gesture desired to be replied by the prosthesis. For this reason, the testing duration is more relevant than the training duration when choosing a classifier for real-time application, however, training time should always be considered.

Cross-validation is, by nature, more computationally demanding and, therefore, more time consuming than train-test evaluation. In our case, a 10-fold cross-validation was iterated 10 times, so the duration of training and testing phases can't be compared to a real-time application. However, the train-test evaluation can. Since the best results were calculated from train-test set 3, this case was used for the training and testing time analysis.

In this train-set set, 25% of the session 2 data set was used as training set and the remaining 75% were used as testing set. Since the data from each session features 400 instances to classify, the training algorithm uses 100 of these instances. Each instance uses 600 ms of gesture related data. This means that the training set corresponds to 60 s of recorded data, which would be a reasonable time to calibrate a myoelectric prosthesis. On the other hand, the testing set corresponds to 300 instances, therefore, 180 s of recorded data.

Considering that train-test set 3 was used, in Table 4.5, the overall average of training and testing time for each of the classifiers in both systems can be observed. The results are presented in milliseconds.

Table 4.5: Overall average of training and testing time for each of the classifiers in both systems, regarding train-test set 3

Classifier	Myo System		OttoBock System	
	Training time (ms)	*Testing time (ms)*	*Training time (ms)*	*Testing time (ms)*
LDA	7986 ± 11072	2196 ± 2831	19308 ± 14351	4742 ± 3385
Linear SVM	437 ± 1036	8 ± 10	857 ± 1345	10 ± 6
Polynomial SVM	32 ± 34	72 ± 78	19 ± 29	32 ± 23
SMO	59 ± 231	8 ± 11	23 ± 11	12 ± 7
Naïve Bayes	10 ± 9	380 ± 358	15 ± 9	779 ± 487
kNN	0	203 ± 182	0	278 ± 183

As it can be observed, the standard deviations reflect the high dispersion of the data. This means the values of time for training and test have a big difference between settings. The main factors that affect these differences are the downsampling and the FFT algorithm application applied to the signal, which affect the amount of data in each instance to classify (the attributes), therefore, affecting computation time.

In most of the presented results, the time values are higher for the OttoBock. This is related with the fact that in settings 1 and 2, a very high sampling frequency was used (1 KHz), compared to the one used in the Myo system (200 Hz), which resulted in more data (or attributes) per instance to classify. However, this allows to observe which classifiers can handle big data sets more efficiently, such as the Polynomial SVM, SMO, naïve Bayes and kNN. On the other hand, classifiers that used linear techniques, such as the LDA and the linear SVM proved to take a greater quantity of time for training with more complex data.

Regarding training time, kNN is the fastest algorithm because it does not require training at all. The neighbours are taken from a set of objects for which the class is known. This can be thought of as the training set for the algorithm, though no explicit training step is required. From the remaining algorithms, Naïve Bayes holds the lower average training time (10±9 ms for the Myo system and 15±9 ms for the OttoBock).

Although kNN and Naïve Bayes have a good performance during the training phase, during the testing phase they are overshadowed by Linear SVM and SMO which provide a much superior performance, providing overall averages of 8±10 ms and 8±11 ms for the Myo system and 10±6 ms and 12±7 ms for the OttoBock, respectively. However, although Linear SVM features similar testing time to SMO, SMO is a more balanced classifier overall. With it, it is possible to calculate high classification accuracies, reduced training time and it is very efficient during testing phase, with an overall average classification rate of about 0.03 ms and 0.04 ms per instance for Myo and OttoBock systems, respectively.

4.3 DISCUSSION

Due to all the signal processing techniques applied and the number of used classifiers, it was possible to get an extensive panoply of results rich in information. Therefore, several conclusions can be taken about the obtained accuracies from each system. The cross-validation results from session 1 will be the first to be analysed.

The cross-validation method was applied on session 1 data set with the purpose to have an idea of its maximum potential for classification. Since in this method all the data is eventually used as training set, it was expected that the results would be better than in the train-test scenario, which was exactly what happened. In the Myo system's case, very high classification accuracies can be observed in setting 2, 4, 6, which all feature low-pass filtration at 1 Hz and signal enveloping. This indicates that the presence of noise has a big influence in classification performance, which might be due to overfitting (read sub-chapter 2.3.5.2). Since the sensors do not provide onboard filtration or enveloping, the results from setting 1, where no signal processing is applied, are very poor. However, just by applying an envelope to the signal and some filtration, accuracies are drastically increased, as observed in setting 2, where the maximum accuracy was 95.72±2.93, using kNN.

The only difference between setting 2 and 4 is that, in setting 4, the signal is downsampled from 200 Hz to 100 Hz, which is half of its original frequency. Despite less data, accuracies did not seem to be affected, as it was proved with paired t-tests between the three best classifiers from both settings. This was to be expected, since the frequencies below 50 Hz are the most relevant to the signal, as observed in the frequency analysis of the sEMG signals acquired. In the settings 2 and 4 from OttoBock system, this can also be verified, despite the sampling frequency difference being even higher (downsampled from 1 KHz to 100 Hz).

Regarding the Myo system, the accuracies from setting 3, where the signal was enveloped, downsampled to 100 Hz and filtered at 45 Hz (to avoid aliasing), show that the enveloping of the signal plays an important role in increasing the classifiers performance, but it is not enough. It is necessary to properly select a cut-off frequency to eliminate most of the noise. Since most of the signal power seems to be concentrated in very low frequencies, 1 Hz was a very appropriate value for the cut-off frequency. This can be justified by observing the difference between the accuracies from setting 3 and 4, where the only difference was the selected cut-off frequency (45 and 1 Hz, respectively)

The effect of proper filtration is evident even in the results from settings 5 (no filtration or enveloping were applied) and 6 (envelope and filtration were applied), where the power spectra were used as features. Setting 6 shows that the use of the signal's frequencies can provide good results and it even calculated the best classification accuracy between all settings: 96.18±2.68%, using kNN.

Now let the focus fall on the results from the OttoBock system for cross-validation. Opposingly to Myo, the results were very similar between all the settings. Very high accuracies can be observed in any situation, even in setting 1, where no signal processing was applied. This justifies why the OttoBock sensors are the standard electrodes used for clinical prosthetic applications. These sensors can indeed provide a high-quality signal due to onboard rectification, filtration, amplification and enveloping. This allows very good classification results, even without any further signal processing. Even after with low-pass filtration at 1 Hz (setting 2), the accuracies are very similar to setting 1, although the maximum setting accuracy suffers a slight increase from 95.70±2.83% to 97.08±2.50% (both with kNN). The latter was found to be the system's maximum accuracy.

The maximum accuracies obtained in each of the systems using cross-validation evaluations (97.08±2.50% and 96.18±2.68%, for the OttoBock and Myo systems, respectively) were compared by means of a paired t-test. The results showed that there were no significant differences between both (p-value = 0.288). Even using the same setting as the one that provided the highest accuracy in the OttoBock system, setting 2, the Myo system can be very competitive (95.72±2.93%, using kNN, as referred before in this discussion).

The results from cross-validation on the session 1 data set showed that, with the right signal processing (and feature extraction), the Myo Armband can reach accuracies just as high as the OttoBock sensors, even just using 5 of its 8 sensors. It is also worth mentioning that the calculated accuracies from both systems had very satisfiable values, nearly reaching the 100% mark. This allowed the validation the main hypothesis of this dissertation, namely the two systems being comparable in performances, and allowed the project to move forward. However, the results from train-test evaluation can be closer to a real-time scenario for the control of a myoelectric prosthesis or a virtual arm. The focus will now fall on the outcome from this evaluation.

As discussed before, the average classifier accuracies from each setting were compared between the three train-test sets used. As it could be observed in Figure 4.10 and 4.11, the average accuracies from both systems have a very noticeable increase between train-test set 1 and 2 and a lower increase between train-test set 2 and 3. In train-test set 1, the data from session 1 is used as training set and the data from session 2 is used for testing. On the other hand, in train-test set 2, 25% from the session 2 data set is added to the data from session 1 for training and the remaining 75% from session 2 is used for testing. The difference between the accuracies from train-test 1 and train-test 2 show that it is better to add data from the present session to the training set than to just use data from a previous session. However, the accuracy differences between train-test set 2 and train-test set 3, which only uses 25% from the present session for training and 75% for testing, show that it is better to delete all data from the previous session and to just use data from the present session for training the classifier. In practical terms, this means that it is better to recalibrate a myoelectric prosthesis when it is taken off and placed again the residual limb. The learning algorithm should be re-trained with new data and forget all the data used for training on a previous session. This is quite justifiable by the fact that when the system is taken off and placed again on the forearm, it is not guaranteed that the sensors will be in the same exact position, therefore the sEMG signals will also have different patterns. This also depends on the way the subject performed the gestures in each of the sessions, the flexion of the wrist might have been different, different levels of force might have been applied, amongst other factors. These are, apparently small differences, but the sEMG patterns are heavily influenced by these factors, which causes the data from one session to be distinctive from another. This directly affects the classifier if the training set contains data from a different session from the data used for the testing set. This could be observed in the results presented. Since the higher accuracies were calculated using train-test set 3, a deeper examination was given to these results.

Observing the accuracies from both systems obtained from train-test 3, it is noticeable that they are lower than the ones observed in the cross-validation evaluation from session 1. This was expected to happen, since the 10-fold cross-validation, in each iteration, divides the data into 10 segments and uses 9 as training set and 1 for testing. This allows the classifier to gather a higher amount of information about the entire data set. However, in train-test evaluation, only a certain percentage of the data set is used as training set. In this particular case, this causes the classification output to be very dependable on how consistent the subject was on performing the hand-gestures. However, in a real-time situation, a solution must be found for the system to deal with slightly different sEMG patterns for the same gesture efficiently. Since each 6 seconds gesture acquisition with steady-state signal was divided into ten 600 ms segments, a solution could be to classify each of these segments and then use a voting system to decide to each gesture the 6 s of data belongs to. Obviously, one could also increase the training set by spending more time acquiring data to train the classifier

Considering the classifier accuracies calculated in each system, shown in Figure 4.13 and 4.17, most of the conclusions drawn for the cross-validation evaluation can be applied in both systems. Considering the Myo systems, the higher accuracies were obtained in settings 2, 4 and 6. Setting 1

provided very poor results and the downsampling did not affect classification accuracy when the signal is enveloped and filtrated. However, the results between classifiers were slightly different. In the cross-validation scenario, kNN provided most the maximum accuracies in each setting, which is no longer true in the train-test evaluation. SMO provided the highest accuracies in all settings, except setting 1, where naïve Bayes outperformed by a long shot all the other classifiers. A non-parametric Friedman test was performed on settings 2, 3 and 4 and it was concluded that the accuracies from SMO were significantly different from the ones calculated by all other classifiers. This classifier achieved the system's overall highest accuracy in setting 2 (88.07±6,87%), followed by setting 4 (86.26±6.31%) and 6 (85.30±5.14%).

Now considering the train-test evaluation results from the OttoBock system, as in the cross-validation scenario, accuracies are very similar between settings but, as in the Myo system's case, classifiers have different performances between them. Polynomial SVM, SMO and kNN seem to produce the best results in all settings, with no significant differences between them. However, in most of the cases, Polynomial SVM provides the higher accuracies and it even obtained the overall maximum in setting 4 (81.85±9.56%), where the signal was downsampled to 100 Hz.

To understand if there were any significant differences between the maximum accuracy obtained in Myo (88.07±6.87%, using SMO) and OttoBock (81.85±9.56%, using Polynomial SVM) systems, a paired t-test was performed. No significant differences were found (p-value = 0.101)

Besides all the discussed results above, a training and testing time analysis was performed to compare the performance of each classifier, in terms of classification duration. Naïve Bayes and kNN seemed to have the best performance during the training phase, however, the time spent in testing is much higher than SMO and Linear SVM. SMO seems to be the classifier that has a better balance between training time, testing time and classification accuracy. This can prove that the usage of the sequential optimization algorithm in SVM is very benefic while classifying sEMG data. From a general point-of-view, SMO provided higher accuracies and less training time than the other two SVM types used (Linear SVM and Polynomial SVM).

Between all the presented results, the classifiers that produced better results were kNN (in cross-validation) and SMO (in train-test evaluation). Polynomial SVM also produced high accuracies for the OttoBock system, in the train-test scenario. However, in every setting, it was not significantly different from SMO or kNN.

Overall, the most important conclusions to take from this preliminary experiment were:

- The Myo system, with the right combination of signal processing techniques and classifiers, can produce classification results as good as the OttoBock system. This is the most important conclusion to take from this experiment because it validates the main hypothesis of this dissertation;
- When the signal is enveloped, and low-pass filtered, the classifier accuracies for the Myo drastically increase;
- In both systems, downsampling the acquired signal to 100 Hz has no influence on classification accuracy, which means the amount of processed data can be lowered and, consequently the classification time;
- Comparing to other accuracies, the ones from settings 3 and 5 were the less interesting. These values were always overshadowed by accuracies from other settings.

- For future experiments, it is relevant to keep setting 1 because, since both sensors are being compared, it is important to have results based on the signal that is outputted directly by the sensor, with no further processing;
- The classifiers that provided the best overall performances were SMO and kNN, for all the reasons stated above.

With the best combinations between signal processing techniques and classifiers chosen and main hypothesis validated, the project could be advanced further by performing sEMG measurements on transradial amputees and comparing the classification results with the achievements from measurements on able-bodied subjects.

5 EXPERIMENT 2: MEASUREMENTS AND COMPARISONS FOR MYOELECTRIC PROSTHESIS CONTROL

The results from the first experiment showed us that the sEMG signals acquired with the Myo system allowed classification accuracies as high as the signals acquired with the OttoBock system. However, all the subjects that participated in this preliminary study were able-bodied. Since the objective is to use these systems for the control of a myoelectric prosthesis, it was essential to measure sEMG signals from the residual limb of subjects with transradial amputation and compare the classification results with the ones obtained from able-bodied subjects. This is the exact purpose of experiment 2.

Experiment 1 also allowed a finer selection of classifiers and signal processing techniques to be used on the data acquired from this new experiment. Also, due to the experience earned during all the measurements performed previously, the used protocol suffered some changes. Due to increased availability of OttoBock electrodes, the number of used sensors in both systems was incremented. The higher number of sensors will allow for a higher quantity of collected data, which is expected to increase the classification performance, since the classifiers will have more information available.

5.1 METHODS

Twelve transradial amputees and twelve able-bodied subjects participated in the task. Each of them gave informed consent before performing the experiment. From the able-bodied subjects, eight of them were male and four were female, with 33.2±11.1 years aged. All of them were healthy, without any muscular or neurological diseases. Regarding the amputated subjects, one of them was female and eleven were male, with 58.3±13.1 years aged. Seven of them suffered the transradial amputation on the right limb and five on the left limb. The years passed since amputation were also registered and can be observed on Table 5.1, along with the age, gender and side of amputation from each amputee.

Table 5.1: Information about the transradial amputees

Subject	Gender	Age	Side of amputation	Years passed since amputation
1	F	52	Right	2
2	M	44	Right	1
3	M	52	Left	14
4	M	70	Left	51
5	M	70	Right	50
6	M	63	Right	49
7	M	45	Left	17
8	M	52	Right	31
9	M	43	Left	1
10	M	67	Left	28
11	M	86	Right	41
12	M	55	Right	38

Regarding the sEMG systems, both populations used setup 2 as described in chapter 3 from this dissertation. Due to the availability of more OttoBock sensors, the total used sensors in both systems were increased to eight, which is the exact of sEMG sensors in the Myo Armband. The sampling rate for the OttoBock system was also altered to 500 Hz. Although the Nyquist Theorem is respected with a 1 KHz sampling frequency, 500 Hz has been proven to be enough for gesture-recognition tasks [53].

In experiment 2, to further explore the potential of the sEMG signals acquired with both systems, the number of hand gestures used for recognition was increased from four to five. The way how each gesture was to be performed also suffered some minor changes. The used hand gestures, which were organized by numbers, are described below:

1. **Rest**: Hand relaxed.
2. **Grasp**: All finger closed, while applying a little amount of force.
3. **Extension**: Hand opened with all the fingers extended.
4. **Indicating**: All fingers closed, except for the extension of the indicator finger.
5. **Pinch**: Indicator and thumb touching, as if picking up a small object.

All the gestures were performed with the forearm leaned on the table.

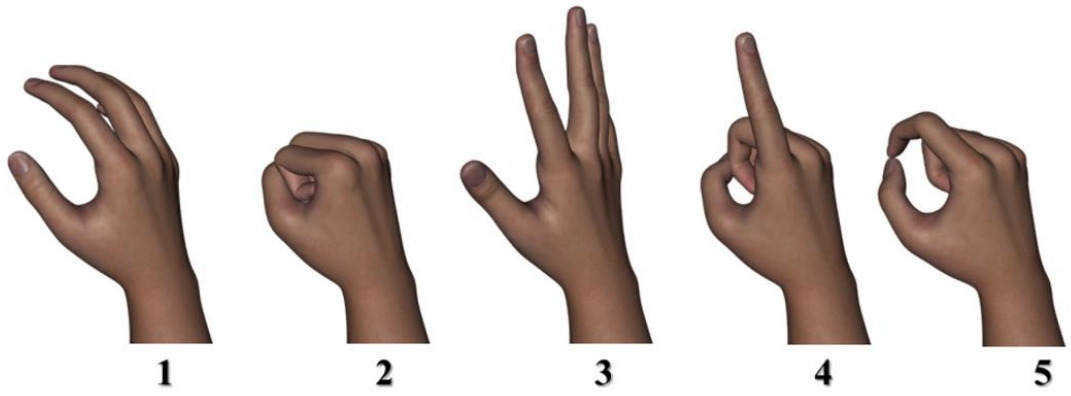

Figure 5.1: The five hand gestures. 1: Rest; 2: Grasp; 3: Extension; 4: Indicating; 5: Pinch. (Adapted from [31])

Each of the gestures was recorded for 2 seconds, 15 times. Acquisitions were made while the subject held the gesture, to record only the steady-state signal. In the case of the able-bodied subjects, each gesture was performed with the right hand. Whereas, amputated subjects were asked to execute the gesture with the phantom limb. The subjects were always instructed when to start performing the hand gesture and when to stop. Between each of the acquisitions, a pause of some seconds would be made, according to the subject's fatigue (more relevant for the amputated subjects).

On able-bodied subjects, both systems were placed on the forearm as in experiment 1, in the mid-point between the elbow and wrist from the right arm. Sensor 1 from both systems was always placed approximately over the *extensor carpi ulnaris*. There was always the attention of placing the sensors of one system, in the same position as the other system's correspondent sensors. In the transradial amputees case, the systems were placed using the same methodology on the residual limb, independently of the side. The only difference is that the systems were placed in the mid-point between the elbow and the most distal portion of the stump.

As in the previous case, this experiment was also divided into two sessions. The protocol used in each of the session was the same and it is described below:

1. The subject is asked to sit on a chair and to get comfortable while the experiment is explained to him/her;
2. Before performing the measurements, sensors from both systems are cleaned using alcohol and a soft tissue;
3. The OttoBock system is placed on the subject's residual limb (or right forearm, in the able-bodied subjects case);
4. 15 acquisitions for gesture 1 are performed;
5. 15 acquisitions for gesture 2 are performed;
6. 15 acquisitions for gesture 3 are performed;
7. 15 acquisitions for gesture 4 are performed;
8. 15 acquisitions for gesture 5 are performed;
9. The OttoBock system is taken off and the Myo System is placed on the same location;
10. Steps 4, 5, 6, 7, 8 are repeated;
11. The Myo system is taken off and the session is over.

The second session was repeated on a different day or, if the subject's availability was limited, it was repeated on the same day.

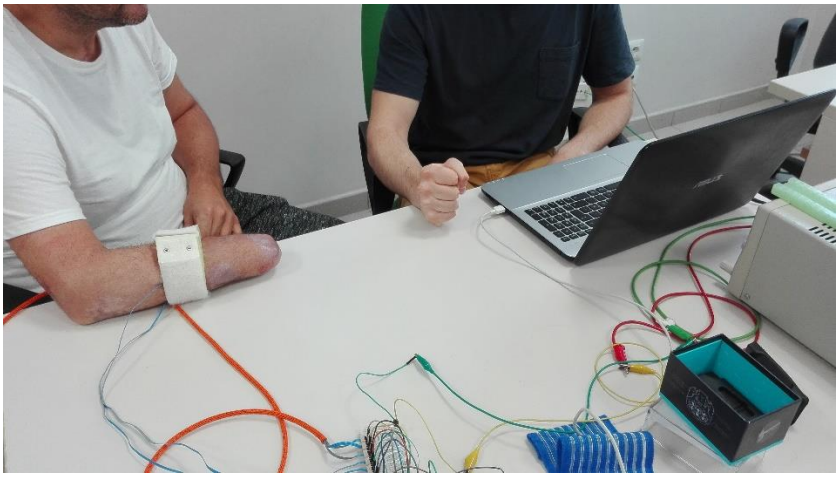

Figure 5.2: Photo taken during one of the sessions with a transradial amputee. For some visual feedback, I always repeated the same gesture with my right hand in each acquisition.

5.1.1 Signal Processing and Feature Extraction

The collected sEMG data was processed in MATLAB, separately for the able-bodied subjects and for the transradial amputees. The data from each subject group was stored in a $[L \times N \times S]$ matrix, where L is the length from the data acquired in each 2 seconds acquisition (400 for the Myo system and 1000 for the OttoBock system, considering each system's sampling frequency), N the number of acquisitions (75) and S the number of used sensors (eight).

The choice of the signal processing techniques to be used in this experiment was based on the results from experiment 1. The results previously presented in section 4.2 showed that settings 1, 2, 4 and 6 produced the higher classification accuracies, considering both systems. The signal processing methods used in these settings will be the ones used in the data acquired in this experiment. To avoid confusion, letters were given to describe each of the settings used in experiment 2:

- **Setting A**: No signal processing was applied to signals from both systems, so the signals were kept "raw", just as they were acquired;
- **Setting B**: The signals from the Myo system were enveloped and a low-pass Chebyshev filter with a cut-off frequency of 1 Hz was applied to the signals from both systems;
- **Setting C**: Data acquired from both sensors was downsampled to 100 Hz and were previously filtered by a Chebyshev low-pass filter with a cut-off frequency of 1 Hz. The signals from the Myo sensors were previously enveloped;
- **Setting D** (described below).

Much like to what was done in experiment 1, each gesture acquisition was divided into 10 segments, each to be used for classification. Each acquisition had a duration of 2 seconds, so each segment had 200 ms, 3 times less than used previously. This leaves us with 750 instances to classify, 150 for each gesture (indeed, each gesture is acquired 15 times and divided into 10 segments). Therefore, there is a higher number of items to classify, with less data in each instance, because the window size selected (200 ms) is less than before (600 ms). Besides, there are also more class labels (five).

The 750 instances from each setting were given directly as input to the classifiers, without any further feature extraction. The only extracted feature was the power spectrum from setting A, using the FFT algorithm on each of the 750 segments. This gives us our last setting, **setting D**.

5.1.2 Classification

Considering the results from experiment 1, the selected classifiers to be used on this experiment were **SMO** and **kNN**, both described previously. Having in account the reduced window length and higher number of instances and used sensors, it will be interesting to observe the results from both classifiers.

Regarding the evaluation of classification accuracy, the same methods from experiment 1 were applied. The data from session 1 was classified using a 10-fold cross validation method, iterated 10 times. On the other hand, for session 2, the classification accuracy was evaluated using the train-test method on the three train-test sets described before:

- **Train-Test set 1**: Training set: Session 1 data set; Testing set: Session 2 data set;
- **Train-Test set 2**: Training set: Session 1 data set, plus 25% of the session 2 data set; Testing set: Remaining 75% from session 2 data set;
- **Train-Test set 3**: Training set: 25% of the session 2 data set; Testing set: Remaining 75% from the session 2 data set.

Overall, two pattern recognition algorithms will be used to classify the data acquired from both systems processed in four distinct ways. Of course, this will be performed for both subject groups: the transradial amputees and able-bodied subjects.

5.2 RESULTS

Throughout this sub-chapter, the classification results from the sEMG data acquired on experiment 2 will be presented and analysed. As in experiment 1, all statistical tests used a 5% significance level. As done previously, the results were also discussed according to accuracy.

5.2.1 10-Fold Cross-Validation Evaluation

This section will start with the observation of the results from the 10-fold cross-validation applied to the data set from session 1. As previously done, first the results from the Myo system will be examined, followed by the results from the OttoBock system.

5.2.1.1 Myo System Results

The average classifier accuracies calculated using the sEMG signals obtained with the Myo system are show in Table 5.2. The results are organized by subject group and setting.

Table 5.2: Cross-validation results from the Myo system: average classifier accuracies, organized by settings, for Amputated and able-bodied subjects.

Average Classifier Accuracies for Amputated and Able-bodied subjects, using the Myo system

Setting	**Amputated Subjects**		**Able-bodied Subjects**	
	SMO	**kNN**	**SMO**	**kNN**
	Accuracy (%)	Accuracy (%)	Accuracy (%)	Accuracy (%)
A	32.84 ± 3.95	22.47 ± 1.74	31.79 ± 4.21	23.23 ± 1.96
B	94.38 ± 2.45	**96.30 ± 1.98**	99.37 ± 0.87	**99.40 ± 0.89**
C	94.17 ± 2.47	96.27 ± 2.02	99.30 ± 0.93	99.39 ± 0.91
D	93.97 ± 2.45	95.68 ± 2.19	98.74 ± 1.18	98.60 ± 1.37

As observed in experiment 1, the average accuracies for setting A are very poor, confirming that, with no signal processing, the signals obtained with the Myo system have no application in classification tasks. On the other hand, for the remaining settings, the results were very satisfying for both subject groups. The accuracies from both classifiers were very similar in each setting. A Wilcoxon Signed-Rank test [59] was made to compare the accuracies from both classifiers in each setting (except for setting A). The results showed that kNN was significantly different from SMO in settings B, C and D from the amputated subjects group, but no significant differences were found in the able-bodied subjects group. In fact, kNN was the classifier that obtained the highest accuracy in each group (96.30±1.98% in the transradial amputees case and 99.40±0.89% for the able-bodied subjects), both in setting B. Using a paired t-test, it was found that these accuracies were significantly different, but by a small margin (p-value = 0.016).

As observed in experiment 1, the results from settings B and C (analogous to settings 2 and 4 from the previous experiment) are practically equal. Besides, the frequency features extracted in setting D proved to obtain very good accuracies.

5.2.1.2 OttoBock System Results

Much like the results from experiment 1, the calculated accuracies with the OttoBock system are very similar between settings, for both subject groups. In Table 5.3 the average classifier accuracies, organized by settings, can be observed. All the accuracies were quite high for both groups, however, the results for able-bodied subjects seemed to be slightly higher.

Table 5.3: Cross-validation results from the Myo system: average classifier accuracies, organized by settings, for Amputated and able-bodied subjects.

Average Classifier Accuracies for Amputated and Able-bodied subjects, using the OttoBock system

Setting	**Amputated Subjects**		**Able-bodied Subjects**	
	SMO	**kNN**	**SMO**	**kNN**
	Accuracy (%)	Accuracy (%)	Accuracy (%)	Accuracy (%)
A	94.97 ± 1.88	94.61 ± 2.33	99.56 ± 0.70	99.63 ± 0.73
B	97.66 ± 1.27	**99.56 ± 0.68**	99.87 ± 0.45	**100.00 ± 0.05**
C	96.74 ± 1.31	**99.55 ± 0.70**	99.72 ± 0.60	**100.00 ± 0.05**
D	96.29 ± 1.36	98.98 ± 1.22	99.71 ± 0.60	99.94 ± 0.29

Like in the Myo system case, to understand which classifier had a better performance, a Wilcoxon Signed-Rank test was made for each pair of classifiers of each setting. In the amputated subjects case, significant differences were found in all settings, except in setting A. On the other hand, for the able-bodied subjects, significant differences were found in setting B and C. However, for all the significant differences found, the p-value, was close to the significance level chosen (0.05). Overall, one could say that kNN had a better performance than SMO, but in practical terms, both classifiers provided very similar results. It was also kNN that provided the best accuracies for both groups, in settings B and C, acquiring almost perfect average accuracies. Both pairs of these accuracies were submitted to a paired t-test and no significant differences were found (p-values were equal to 0.340 and 0.266, respectively).

5.2.2 Train-Test Evaluation

5.2.2.1 Myo System Results

Let one now consider the results obtained using train-test evaluation on train-test sets 1, 2 and 3, shown in Table 5.4, 5.5 and 5.6, respectively. Once again, the train-test set 3 features the highest accuracies. However, the results are very similar to train-test set 2, as it can be observed in Figure 5.3, where the total average between both classifiers are represented by setting, for each train-test set. The lines that represent train-test set 2 and 3 are practically overlapped. The main difference between both

sets is that train-test set 2 uses all the data set from session 1, plus 25% of session 2 as training set and train-test 3 uses only 25% of session 2. Therefore, train-test set 3 allows us to get accuracies as high as the ones from train-test set 2 using less data for training. This issue has been addressed before in experiment 1. Taking this into account, train-test set 3 was analysed more thoroughly.

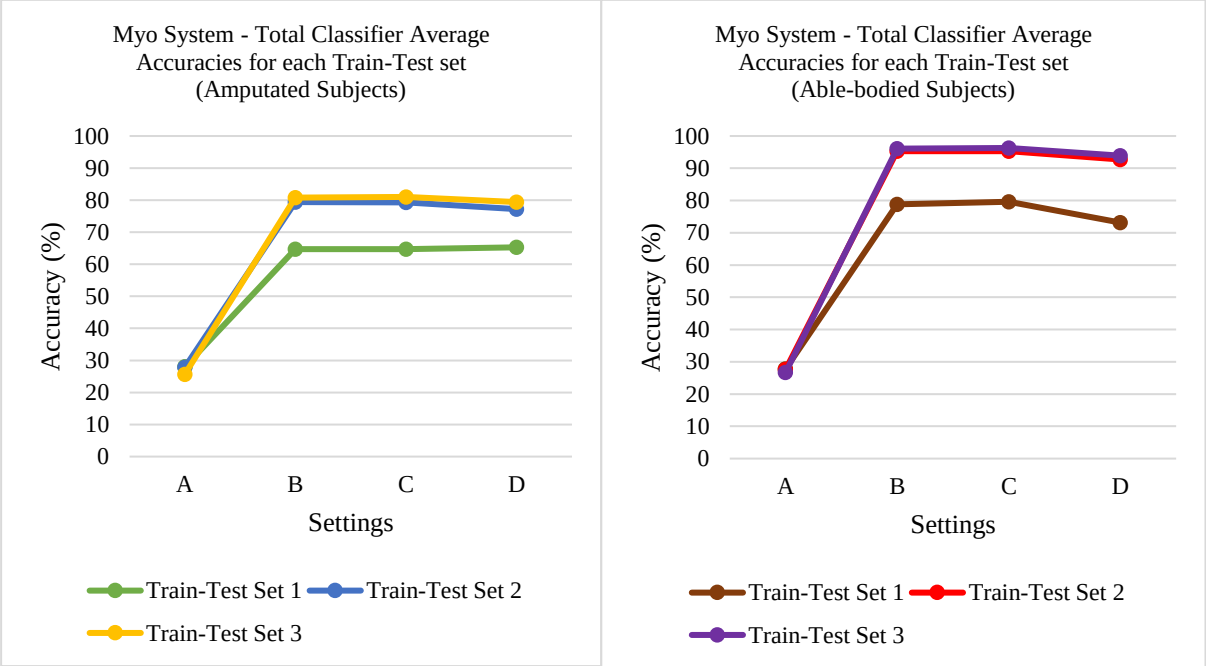

Figure 5.3: Total Classifier Average Accuracies for each Train-Test set, using Myo system. In the left: results from the amputated subjects; In the right: results from the able-bodied subjects

Considering only train-test set 3, at first glance, it is obvious that higher average accuracies were obtained for the able-bodied subjects, which are in the order of 90% for settings B, C and D. Instead, the calculated accuracies for the amputated subjects were around 80% for the same settings.

Once again, settings B, C and D featured very similar performances between each other, in both subject groups. As done in the cross-validation evaluation case, a Wilcoxon Signed-Rank test was made for each pair of classifiers of these settings. The results showed no significant differences between SMO and kNN. However, SMO produced the highest average accuracies in each subject group, achieving 81.58±10.17% for the transradial amputees case and 96.49±2.90%, both in setting C. These average accuracies proved to be significantly different by means of a paired t-test (p-value = 0.001). In the light of this information, it can be stated that the signals extracted from able-bodied subjects were able to provide a better classification accuracy.

Table 5.4: Train-test evaluation results from the Myo system, using train-test set 1: average classifier accuracies, organized by settings, for amputated and able-bodied subjects.

Results from Train-Test set 1: Average Classifier Accuracies for Amputated and Able-bodied subjects, using the Myo system

Setting	**Amputated Subjects**		**Able-bodied Subjects**	
	SMO	**kNN**	**SMO**	**kNN**
	Accuracy (%)	Accuracy (%)	Accuracy (%)	Accuracy (%)
A	32.73 ± 4.13	23.34 ± 3.62	31.82 ± 3.83	23.71 ± 3.56
B	63.43 ± 19.28	66.03 ± 19.72	78.79 ± 18.68	78.90 ± 20.57
C	63.56 ± 19.29	65.90 ± 19.70	**80.36 ± 16.86**	78.87 ± 20.54
D	64.04 ± 17.90	**66.50 ± 19.04**	72.61 ± 16.76	73.68 ± 21.57

Table 5.5: Train-test evaluation results from the Myo system, using train-test set 2: average classifier accuracies, organized by settings, for amputated and able-bodied subjects.

Results from Train-Test set 2: Average Classifier Accuracies for Amputated and Able-bodied subjects, using the Myo system

Setting	**Amputated Subjects**		**Able-bodied Subjects**	
	SMO	**kNN**	**SMO**	**kNN**
	Accuracy (%)	Accuracy (%)	Accuracy (%)	Accuracy (%)
A	32.80 ± 3.66	22.95 ± 3.82	32.16 ± 2.80	23.00 ± 2.96
B	79.26 ± 16.86	**79.52 ± 12.80**	94.91 ± 5.57	**95.64 ± 2.75**
C	79.21 ± 16.61	79.37 ± 12.87	95.00 ± 5.49	95.58 ± 2.73
D	78.38 ± 17.28	76.08 ± 16.07	92.41 ± 6.60	93.02 ± 3.11

Table 5.6: Train-test evaluation results from the Myo system, using train-test set 3: average classifier accuracies, organized by settings, for amputated and able-bodied subjects.

Results from Train-Test set 3: Average Classifier Accuracies for Amputated and Able-bodied subjects, using the Myo system

Setting	**Amputated Subjects**		**Able-bodied Subjects**	
	SMO	**kNN**	**SMO**	**kNN**
	Accuracy (%)	Accuracy (%)	Accuracy (%)	Accuracy (%)
A	31.24 ± 2.73	20.17 ± 1.00	30.71 ± 2.46	22.64 ± 4.92
B	81.14 ± 10.34	80.43 ± 10.83	96.01 ± 3.62	96.13 ± 3.17
C	**81.58 ± 10.17**	80.40 ± 10.85	**96.49 ± 2.90**	96.09 ± 3.21
D	80.92 ± 11.90	77.89 ± 13.41	94.37 ± 3.24	93.52 ± 3.35

5.2.2.2 OttoBock System Results

What was observed in the Myo system's case is analogous for the OttoBock system. As it can be observed in Figure 5.4, the total averages from train-test sets 2 and 3 are, by far, superior to the ones form train-test set 1. The accuracies between train-test 2 and 3 are also very similar, however, as observed before, it is more practical to use data from the present session as training set, instead of adding data from a previous session.

By observing the results from train-test set 3, in Table 5.9, at first sight, SMO seemed to produce the highest accuracies once again. As usual, a Wilcoxon Signed-Rank test was made for each pair of classifiers of these settings. The results from these tests showed no significant differences between the classifiers except in setting A from the able-bodied subjects group. In fact, in this setting SMO obtained the highest average accuracy for the same group: 94.57±4.22% (in setting A). Additionally, SMO also calculated the highest average accuracy for the amputated subjects group: 87.08±9.06% (in setting C). The highest average accuracies from both groups were proven to be significantly different, by means of a paired t-test (p-value = 0.001).

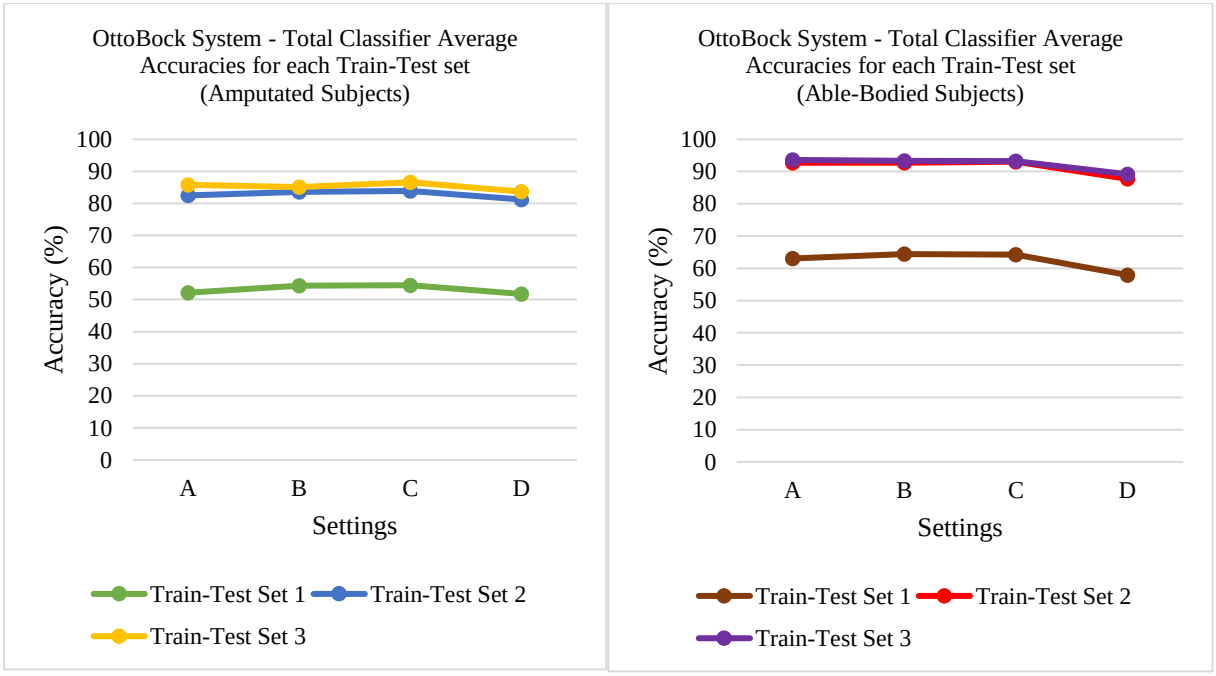

Figure 5.4: Total Classifier Average Accuracies for each Train-Test set, using OttoBock system. In the left: results from the amputated subjects; In the right: results from the able-bodied subjects

Table 5.7: Train-test evaluation results from the OttoBock system, using train-test set 1: average classifier accuracies, organized by settings, for amputated and able-bodied subjects.

Results from Train-Test set 1: Average Classifier Accuracies for Amputated and Able-bodied subjects, using the OttoBock system

Setting	**Amputated Subjects**		**Able-bodied Subjects**	
	SMO	**kNN**	**SMO**	**kNN**
	Accuracy (%)	Accuracy (%)	Accuracy (%)	Accuracy (%)
A	49.51 ± 13.93	54.78 ± 17.48	61.62 ± 21.83	64.47 ± 17.54
B	52.24 ± 12.55	56.44 ± 15.67	64.31 ± 22.05	64.51 ± 18.83
C	52.49 ± 12.31	**56.48 ± 15.63**	63.92 ± 22.73	**64.54 ± 18.84**
D	50.48 ± 12.75	53.03 ± 15.27	56.49 ± 22.31	59.40 ± 18.08

Table 5.8: Train-test evaluation results from the OttoBock system, using train-test set 2: average classifier accuracies, organized by settings, for amputated and able-bodied subjects.

Results from Train-Test set 2: Average Classifier Accuracies for Amputated and Able-bodied subjects, using the OttoBock system

Setting	**Amputated Subjects**		**Able-bodied Subjects**	
	SMO	**kNN**	**SMO**	**kNN**
	Accuracy (%)	Accuracy (%)	Accuracy (%)	Accuracy (%)
A	82.10 ± 11.73	82.92 ± 9.26	92.85 ± 6.18	92.67 ±5.79
B	83.20 ± 11.83	84.05 ± 9.19	93.12 ± 5.91	92.42 ± 5.74
C	83.70 ± 11.30	**84.07 ± 9.22**	**93.71 ± 5.98**	92.42 ± 5.73
D	81.17 ± 10.87	81.26 ± 8.26	87.46 ± 7.78	88.00 ± 7.07

Table 5.9: Train-test evaluation results from the OttoBock system, using train-test set 3: average classifier accuracies, organized by settings, for amputated and able-bodied subjects.

Results from Train-Test set 3: Average Classifier Accuracies for Amputated and Able-bodied subjects, using the OttoBock system

Setting	**Amputated Subjects**		**Able-bodied Subjects**	
	SMO	**kNN**	**SMO**	**kNN**
	Accuracy (%)	Accuracy (%)	Accuracy (%)	Accuracy (%)
A	85.93 ± 9.68	85.59 ± 8.91	**94.57 ± 4.22**	92.65 ± 5.83
B	84.05 ± 8.80	86.11 ± 9.89	94.11 ± 4.76	92.60 ± 6.08
C	**87.08 ± 9.06**	86.12 ± 9.89	93.82 ± 4.85	92.59 ± 6.09
D	84.05 ± 8.80	83.30 ± 9.42	90.20 ± 5.73	88.14 ± 7.15

5.2.3 Effect of Time Passed Since Amputation

It was hypothesised that the time that passed since amputation could have some influence over the classification accuracy. With the passing of the years, a subject with transradial amputation does not use his phantom limb for any task. This can make the subject "forget" how to do a certain gesture with the phantom hand, which could have affected the presented results. In fact, several of the amputated subjects that participated in this experiment, before the beginning of each session, had some difficulty imagining some of the hand gestures asked to perform. The "hardest" gestures for most of the amputees were gestures 4 and 5, the "pointing" and the "pinch".

To understand if there could exist linear correlation between these two variables, the number of years passed since amputation was confronted with the accuracies obtained with SMO in setting 3, which was the setting that provided the highest accuracies for transradial amputees in both systems. The results from train-test evaluation in train-test set 3 were used for this task because it is the scenario closer to a real-time application of the systems for the control of a myoelectrical prosthesis. The results from both systems are shown in the scatterplots from Figure 5.5.

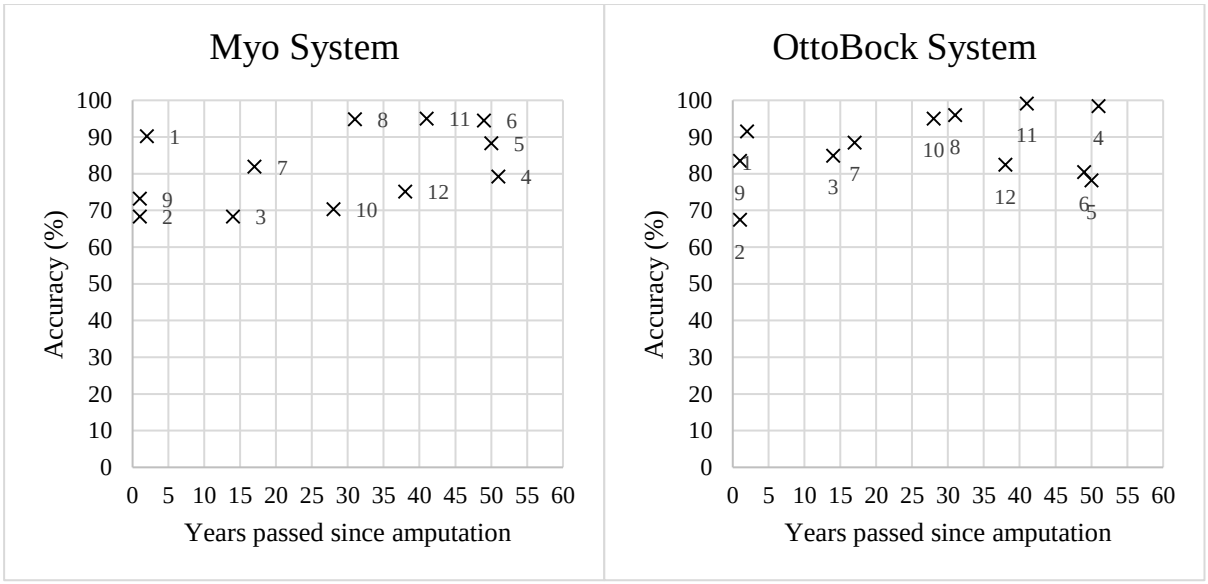

Figure 5.5: Scatterplots showing the best accuracies obtained from train-test set 3 vs the years passed since the amputation of each transradial amputee. In the left: results from the Myo system; In the right: results from the OttoBock system. The number next to each of the crosses represents the subject's number

The expected outcome was to observe an inversely proportional relation between accuracy and the years passed since amputation. Instead, the results from the scatterplots showed that there is no correlation between these two variables. The Pearson correlation coefficient (r), which measures the linear correlation between two variables, was also calculated for both cases. Both in OttoBock and Myo systems, no significant linear correlation was detected (r = 0.291 and r = 0.465, respectively). This means that the number of years past since amputation do not affect the possibility for the amputee to use a sEMG system, such as the ones presented in this dissertation, to control a myoelectric prosthesis.

5.3 DISCUSSION

From a general point of view, the increased number of sensors allowed for better accuracies than in experiment 1, despite the increment in the number of used hand gestures and instances to classify. The smaller window length (200 ms) also showed to produce a good performance in both systems.

Regarding the cross-validation evaluation done in the session 1 data set, the calculated accuracies from both subject groups were quite high in each of the sEMG systems, except in setting A from the Myo system where no signal processing was applied. These accuracies were always slightly higher for the able-bodied subjects. However, the amputated subjects group produced very competitive accuracies in both systems. In the Myo system's case, the highest accuracies from both groups were found to be significantly different, but for a very small margin (p-value = 0.016). On the other hand, for the OttoBock system, no significant differences were detected. Therefore, according to the cross-validation evaluation, a transradial amputee can have a performance as good as an able-bodied subject while using a sEMG system for the recognition of hand-gestures.

In both subject groups, considering the two systems, the highest accuracies were found to be calculated using setting B with the kNN classifier. Although the accuracies from setting B were the highest, they are not significantly different from the ones calculated in setting C, in fact, they are practically equal. This shows once again that downsampling signals from both systems to a 100 Hz sampling frequency, has no effect in classification performance, even with a smaller window length. This allows classification with much lesser data, which makes its computation time more reduced and efficient.

About differences between the sEMG systems regarding the cross-validation evaluation, at first sight, the accuracies calculated with the OttoBock system seem to be slightly higher than the ones from the Myo system. A paired t-test was made between the highest accuracies from both systems, separately for the amputated and able-bodied subjects. The used accuracies were from setting B, obtained with kNN, which featured the highest accuracies in both systems, as stated above. The results from this statistical test showed that there were significant differences for both amputated (p-value = 0.002) and able-bodied (p-value = 0.007) subject groups. However, although the OttoBock system provided better accuracies, the Myo system is not far behind.

Now considering the train-test evaluation results, as done in experiment 1, this evaluation was applied to three different combinations of training and testing sets, given the name of "train-test sets". The highest accuracies in every case seemed to be calculated with train-test 2 and 3. Train-test set 1, as in experiment 1, featured very poor accuracies, when comparing to the other sets. Once again, it is proven that the usage of data from a previous session as training set and data from the present one for testing is not a good approach for classification. However, when added 25% from the present session to the training set, the classifier accuracies have a substantial increase, as observed with train-test set 2. In this experiment it is interesting to observe how similar the results of train-test set 2 and 3 are. However, as discussed before, if the results are not significantly different, there is no point in using data from both sessions and load the classifier with a higher burden than it should. Besides the changes made in the protocol and to the systems, the following conclusions from experiment 1 remains valid: each time the system is taken off and placed again, it is preferable to retrain the classifier with new data. In practical terms, this translates to a full recalibration of the myoelectric prosthesis.

Concentrating now on the results from train-test evaluation on train-test set 3, comparing to the results from cross-validation, the accuracies were lower, as it was expected. However, very satisfiable

accuracies were obtained for the able-bodied subjects, which were significantly higher than the accuracies calculated from the transradial amputees, as observed in the results section. There are several reasons why the accuracies were lower for the transradial amputees. For instance, the replication of hand gestures requires a higher level of concentration because the subject must imagine how to do them with the phantom hand. This can cause the subject to perform the gesture in an inconsistent way throughout the session, therefore the signals from the last acquisitions can be slightly differently from the first ones, causing this discrepancy on the accuracies. Although it was asked to each subject to apply the same level of force to each gesture, there might have been some force variations throughout the session that affected the classifiers performance. Also, after the amputation, the muscle conformation becomes slightly different, which can also have some effect on the accuracies. Despite these setbacks, a maximum average accuracy of 81.58±10.17% and 87.08±9.06% were calculated, with the Myo and OttoBock systems, respectively. Both these accuracies were obtained using SMO on setting C. As usual, a paired t-test was performed to understand if there were any significant differences between the highest accuracies from both systems, for the transradial amputees. Although the maximum accuracy calculated with the OttoBock system is higher than the one calculated with the Myo system, no significant differences were found (p-value = 0.121).

On the other hand, the accuracies calculated in the able-bodied subjects group were comparable to the ones calculated in cross-validation evaluation. Using just 25% of the present session as training set is the equivalent of spending approximately 37.5 seconds (25% of the 750 instances to classify times the window length, 200 ms) to calibrate the system, which is a very acceptable time window to calibrate a myoelectric prosthesis.

The highest accuracies for the able-bodied subjects group were found to be 96.49±2.90% (using SMO on setting C) and 94.57±4.22% (using SMO on setting A) for the Myo and OttoBock respectively. As in the transradial amputees case, no significant differences were found between these accuracies (p-value = 0.215, using a paired t-test). As in the previous experiment, it is interesting to observe the good performance of the OttoBock system using setting A, where no signal processing was applied. Once again, this shows the high quality of the output signal from the OttoBock sensors.

In terms of the used classifiers, from a general point of view, kNN provided the best accuracies in cross-validation evaluation. On the other hand, SMO provided the highest accuracies in train-test evaluation on train-test 3, however, with no significant differences from kNN in most cases. Since the train-test evaluation is the most comparable to a real-time situation, SMO would be the best classifier to use, not only by the high calculated accuracies, but for the reduced classification time during the testing phase, which was observed to be lesser than kNN in experiment 1. This would make the usage of these systems in real-time much more computationally efficient.

Other interesting results were shown in the analysis made about the effect of time passed since amputation on the amputated subjects performance. Since no correlation was detected between these two variables, one can point out that the years that passed since amputation do not affect the possibility of the amputee to use a myoelectrical prosthesis that uses gesture recognition. As pointed out before, this could have been a problem because with the passing of the years, the amputee has more and more difficulty in imagining more complex hand gestures, such as “pointing” and the “pinch” gestures used in the experiment. However, from a classification point of view, the most important aspect is that the signals generated by the residual limb’s muscle are distinct from each other and that the gesture is performed in the same way during each acquisition.

Overall the main conclusions to take from this experiment were the following:

- The cross-validation evaluation results from both systems showed a significant difference between the Myo and OttoBock system's calculated accuracies, showing that the latter had a better overall performance. However, the accuracies obtained using the Myo system provided very competitive results and very high classification accuracies, for both amputated and able-bodied subjects groups;
- It is better to use data from the present session to train the classifier than use data from the previous;
- The train-test evaluation on train-test 3 is closer to e real-time application. The results between both sEMG systems showed no significant difference, for both transradial amputees and able-bodied subjects, which validates the main hypothesis of this dissertation: the Myo system can provide a performance as good as the OttoBock system for the control of a myoelectric prosthesis;
- From a general point of view, the accuracies for able-bodied subjects were significantly higher than the ones for transradial amputees;
- The best classifier for real-time application is the SMO, although kNN provides significantly better results in cross-validation evaluation;
- The years passed since amputation do not affect the possibility of a transradial amputee to use a myoelectrical prosthesis with gesture recognition.

As a final remark, the author would like to add that the stay at INAIL prosthesis centre provided the unique opportunity to observe how different kinds of prosthesis were built and to observe myoelectric prosthesis being used by amputees, amongst them, the Michelangelo hand, which is one of the most advanced myoelectric prosthesis in the market, as referred before in this dissertation. Besides, every session with the transradial amputated subjects was definitely a very positive experience. Every single one of them showed no problem in spending some time taking measurements and were happy that they could help develop this dissertation. The good mood present throughout each session made all the time spent performing acquisitions much more enjoyable. However, the best outcome from this experiment was to know that, after each session, some subjects felt a decrease of the pain felt in the phantom limb (PLP) and even referred they would try to do something similar at home. To know that this experiment could have such a positive effect on some people that suffered a transradial amputation was, without a doubt, the best direct result the author of this dissertation could hope for.

6 CONCLUSIONS

At the beginning of this dissertation it was discussed the high costs that a transradial amputee must pay for a myoelectric prosthesis. Living with the loss of a hand affects directly most of daily tasks that one takes for granted. A device such as this type of prostheses can replace some of the functions from the missing limb and restore some of the amputee's quality of life. Therefore, it is paramount that every individual living with amputation can have access to quality myoelectric protheses at an accessible price. There have been some approaches to reduce these costs, such as the 3D printing of some components [33] [34]. However, the performance of a myoelectric prosthesis also depends from the quality of the sEMG signals acquired from the remaining muscles in the residual limb, especially if it uses hand gesture recognition. In such type of prosthesis, the acquired signal is then processed, features are extracted and given as input to pattern recognition algorithms called classifiers. Roughly speaking, classifiers, in this situation, try to guess to which hand gesture certain sEMG patterns belong to, therefore, it is imperative to have a quality signal for getting good classifying accuracies. For this end, it is required to use quality sEMG sensors, which can increase drastically the price of the device. However, in terms of classification for the controlling of a myoelectric prosthesis, how much is the real difference between low-cost and high-end sensors?

It was hypothesized if low-cost sensors could have a performance for the control of a myoelectric prosthetics as good, or even superior to high-end sensors. To test this hypothesis, two different systems were used. One of these systems was built during my stay in University of Rome "Tor Vergata" and used sensors from OttoBock, which are the standard ones for prosthetic applications. Each of these sensors has an approximate cost of $400 each (total cost for the whole system equal to $3,200, without considering the elastic band and the data acquisition and transmission hardware components). The other used system was the Myo armband, a low-cost commercial bracelet that features eight sEMG sensors and has the cost of $199, which is much lower than a single OttoBock sensor. Both systems can be applied to control a gesture-based myoelectrical prosthesis. Based on this assumption, the Myo and OttoBock systems were used to make sEMG measurements on able-bodied subjects and transradial amputees. The data acquired was then used for classification and the calculated classification accuracies were compared between systems. If no significant differences could be found, then the main hypothesis of this dissertation would be validated. This could mean that there is the possibility to build myoelectrical prostheses at lower prices and with the same performance quality as the ones that use high-end sensors, such as the OttoBock ones.

To select the best signal processing techniques and classifiers to be used, a preliminary experiment was performed on nine able-bodied subjects. This experiment was also done to validate the main hypothesis presented before moving on to perform measurements on transradial amputees. On this experiment, "experiment 1", four different hand gestures (rest, grasp, extension and pinch) were recorded continuously. Data was recorded throughout two sessions. In each session, each gesture was recorded for 10 seconds, 10 times, for each system. After all the recording was done, a frequency analysis was performed on the acquired signals. This allowed the selection of frequency values for filtering and for downsampling to be used in the different signal processing techniques applied. In total, six different combinations were used, featuring low-pass filtering at 1 Hz and downsampling the sampling frequency to 100 Hz. These signal processing combinations were given the name of "settings". No feature extraction was used, except for the use of FFT on two of the settings. The reduced use of features is justified by the wish to compare directly the signals acquired from both sensor types by means of classification. Only the last 6 seconds from the recording of each gesture were used, to avoid the

transient signal and use only the steady-state one. A window length of 600 ms was used with no overlapping.

The results from experiment 1 showed that, considering the maximum average accuracies obtained in each system, no significant differences were found, considering cross-validation and train-test evaluation. This obviously validated the main hypothesis and allowed the rest of the project to carry on. However other important conclusions were drawn.

When no signal processing is applied to the signals from the Myo system, the accuracies are poor, however, when the signal is enveloped and filtered with a Chebyshev filter with a cut-off frequency of 1 Hz, the calculated accuracies have a dramatic increase and become very competitive with the accuracies obtained using the OttoBock system. The latter, on the other hand, provides very satisfiable accuracies, even without any signal processing. The signal is enveloped and filtered inside the sensor, which justifies why the obtained signals provide such a good classification performance.

In both systems, when the signal is enveloped and filtered at 1 Hz, it provides practically equal results to when the same signal is downsampled to 100 Hz. This was expected because in the frequency analysis, we could observe that most of the signal's power was concentrated in frequencies below 50 Hz, especially near 0 Hz. This was an important result, because it allowed to calculate the same level of accuracies but with less data, which lessens the computational burden of the classifier.

It could be also observed in train-test evaluation that it is better to use data from the present session to train the classifier than to use data from a previous session. This is a very relevant point, because it means that a myoelectrical prosthesis that uses this type of systems for its control requires the retraining of the classifier with new data each time it is taken off and placed again on the residual limb.

Overall, considering only five sensors were used in each system, the maximum calculated accuracies were satisfiable. In cross-validation evaluation applied to the first session, a maximum of 96.18±2.68% and 97.08±2.50% average accuracies were reached, for Myo and OttoBock system, respectively. On the other hand, the train-test evaluation on train-test 3, using the data from the second session, allowed to calculate a maximum of 88.07±6.87% and 81.85±9.56%, for Myo and OttoBock systems, respectively.

This first experiment also allowed to select the best settings and classifiers to be used on the second experiment. From a general point of view, SMO and kNN allowed to calculate the best accuracies in both evaluations and sessions.

With the main hypothesis validated, along with best performing classifiers and settings selected, it was time to move to the next experiment. In experiment 2, sEMG measurements were performed on twelve transradial amputees and twelve able-bodies subjects. Only four from the six settings used experiment 1 were selected, along with only two classifiers, SMO and kNN.

This time, eight sensors were used in both systems and the used protocol suffered some changes. Fifteen repetitions of 2 seconds acquisitions for each of five gestures (rest, grasp, extension, indicating and pinch) were performed for each subject, acquiring only the steady-state signal. The window length used was of 200 ms with no overlapping.

The results from the cross-validation on data from the first session showed significant differences between the systems, meaning that the OttoBock system had the best performance for both types of subjects. However, the accuracies calculated by the Myo system showed to be extremely competitive, acquiring a maximum average of 96.30±1.98% for the transradial amputees and 99.40±0.89% for the able-bodied subjects.

Considering the results from the train-test evaluation on train-test set 3, no significant differences were found between both systems. Since this evaluation might be closer to a real-time scenario, such as the application to an myoelectrical prosthesis, this can validate the main hypothesis.

The obtained accuracies of both systems showed that able-bodied subjects had a better performance than transradial amputees, which was to be expected. Due to the low use of muscles from the residual limb, the way some hand gestures are performed becomes more difficult to imagine and remember for the amputated subjects. The lack of visual feedback can also have some impact on the performances. However, the results do not discard the possibility for transradial amputees to use this kind of systems to control a gesture-based myoelectric prosthesis. It was also shown that the time passed since the amputation does not affect the subject's performance, which means it does not affect possibility of the subject to use such devices.

Considering the average accuracies from able-bodied subjects, they were higher than in the previous experiment, nearly reaching 100%. This is obviously due to the increase in the number of sensors. Extra sensors in different positions from the forearm provide a signal richer in information, which reflects in the classifier's performance. The remaining conclusions taken from this experiment were analogous to experiment 1.

Overall, it is possible to conclude that low-cost sensors, such as the ones from Myo armband, can provide classification results as good as high-end sensors, such as the OttoBock sensors. This means that this type of low-cost sensors can be used to control a myoelectric prosthesis and deliver a performance as good as a system using more expensive sensors. This can help, in fact, reducing the costs for the final user, the transradial amputee, while maintaining performance quality. However, as observed, it is necessary to apply the right signal processing techniques to the signal, because with no signal processing at all, the results can be quite poor. This is the main difference between both type of sensors, the OttoBock sensors justify the reason of being so widely used in prosthetic application because the acquired signal is ready for classification purposes.

Just by applying an envelope and low-pass filtering at 1Hz, the signals acquired with the Myo sensors provide drastically higher classification accuracies, which, as observed, do not have any significant differences from the results calculated with OttoBock sensors. Perhaps, instead of digitally, this can be applied in a circuit interface with the Myo sensors. This could be done to reduce the computation time when used in a real-time situation. It was also shown that the feature extraction used offered no further advantages over using no feature extraction at all.

Perhaps one of the most interesting results was to observe that the signal downsampled to a 100 Hz sampling frequency, along with the application of an envelope and filtration, allowed practically equal accuracies to the ones calculated with the signals original frequency, which in the Myo system's case was the double: 200 Hz. In a real-time system, perhaps this could be the best signal processing to use, along with SMO, which was proven to be very fast in classifying data during the testing phase.

Considering the train-test evaluation, the obtained accuracies in train-test set 2 and 3 were similar in both experiments. Although the accuracies calculated in train-test set 3 were slightly higher and deserved a deeper analysis, the results from train-test set 2 can also prove to be useful for prosthetic applications. In train-test set 2, it was observed that adding training data from the present session to training data from a previous session substantially increased obtained accuracies. Perhaps, a myoelectric system could be recalibrated using data from a previous session as training set plus a reduced quantity of data from the present session by only using only one or two of the selected hand gestures for calibration, with less repetitions. An auto-learning algorithm could be implemented to use the data from

the correctly identified gestures to further improve the subsequent accuracies and overall performance of the system. This way, the myoelectrical prosthesis would feature a very fast calibration without the necessity of making the classifier relearn data from scratch. However, first it would be necessary to understand if there is a gesture or a subset of gestures that can fully characterize the system.

The focus in this dissertation was to compare both sensors based on classification accuracy. However, when such systems are applied to a real-time system, misclassification must be considered. In this case a wrongly classified instance can lead to wrong classification-based decision, which can originate accidents if the task being made requires some precision. When it comes to myoelectric prosthesis, it is imperative that no mistakes can be permitted. For this reason, it is preferable for the classifier to abstain instead of misclassifying an instance. This can be done by using a voting system between classes obtained between contiguous windows. If, during a selected time interval, the number of instances classified with a certain class label reaches a chosen threshold, then the prosthesis executes the hand gesture correspondent to that label. On the other hand, if the threshold is not reached, then no action should be executed by the prosthesis. In a nutshell, the robustness of this type of control system is more important than high accuracies. This is an issue that is many times overlooked in this research area but that should always be considered when designing a myoelectric prosthesis. Good communication between the device's functionalities and the user's intentions is the key.

Besides, throughout this dissertation, only the steady-state sEMG signal was used for classification purposes. In a real-time application, the transient signal must be considered. The presence of this signal can reduce the obtained accuracies and decrease the overall performance.

As observed in experiment 1, using only five sensors can also produce high classification accuracy. To further decrease the cost of myoelectric prostheses, less sensors can be used, if no significant differences are detected between the chosen number of sensors and the ones currently being used. Such study can be made to understand which are the optimal positions in the forearm to place the sensors. Such "optimal positions" should provide more distinctive sEMG patterns between different hand gestures. However, every human being is different, which means that, unfortunately, no optimal sensor positions can be applied in a generalized way. Muscle size, forearm diameter, amongst other factors can change from individual to individual, which obviously limits the selection of a predefined sensor positioning that can provide the same performance for every individual, while controlling a myoelectrical prosthesis.

Although the issues referred above, the results presented throughout this dissertation are encouraging for further research and hopefully can help provide conditions for the manufacturing of myoelectric prosthesis with lower final costs. The best result to hope for is to create a positive impact on the lives of transradial amputees and try to restore the functionalities from the missing limb without having to pay an excessive price for it. Myoelectric prosthesis can provide a huge improvement in the quality of life; therefore, it is essential that they can be accessible for everyone.

6.1 FUTURE WORK

In this dissertation, it was proven that, the use of low-cost sensors in a sEMG system can provide results that, from a classification point of view, are as good as the ones obtained with a system using high-end sensors. However, this is just a scratch in the surface before it can be applied to an actual myoelectric prosthesis. Some of the future work related with this project will have to face challenges,

such as the application of these systems in a real-time scenario. Something close to the experiments conducted in this work, but with real-time classification. Besides, a solution must be engineered for the solving of the misclassification problem. If the classifier is not sure of the class label for a certain instance, it is better to just abstain. Decreasing the number of used sensors must be also considered. This way, the final cost of such a system can be further decreased. Finally, the optimized system must be tested for the control of an actual myoelectric prosthesis.

Throughout this dissertation, the analysis performed had always in consideration the application of these systems to a myoelectric prosthesis, however it can have other interesting applications, such as the use in the therapy. As stated before, PLP can be reduced if the amputee can have some visual feedback while using a sEMG system. This can be done by using the presented systems for the control of a representation of the missing limb in a virtual environment. In this case classification should be performed in real time and each class label would correspond to a different limb position or hand gesture.

Furthermore, as discussed in chapter 2, these systems can also have other interesting applications, such as sign language recognition, the control of an exoskeleton or even for *gaming*.

7 BIBLIOGRAPHY

[1] W.R. Frontera, J.K. Silver. "Fondamenti di Medicina Fisica e Riabilitativa". Rome, Verducci Editore, 2014.

[2] K. Ziegler-Graham, E.J. MacKenzie, P.L. Ephraim, T.G. Travison, R. Brookmeyer. "Estimating the Prevalence of Limb Loss in the United States: 2005 to 2050". Archives of Physical Medicine and Rehabilitation, 2016.

[3] M. Owings, L.J. Kozak. "Ambulatory and Inpatient Procedures in the United States". National Center for Health Statistics, 1996.

[4] F. Cordella, A.L. Ciancio, R. Sacchetti, A. Davalli, A.G. Cutti, E. Guglielmelli, L. Zollo. "Literature Review on Needs of Upper Limb Prosthesis Users". Frontiers in Neuroscience, 2016.

[5] H. Flor. "Phantom Limb Pain". Elsevier, 2008.

[6] L. Nikolajsen, T.S. Jensen. "Phantom Limb Pain". British Journal of Anaesthesia, 2001.

[7] N. Jiang, S. Dosen, K.R. Müller, D. Farina. "Myoelectric Control of Artificial Limbs-Is there a Need to Change Focus?". IEEE Signal Processing Magazine, 2012.

[8] E. R. Ramírez. "Control of a hand prosthesis using mixed electromyography and pressure sensing". Master's thesis, Escola Tècnica Superior d'Enginyeria Industrial de Barcelona, 2016.

[9] F. Cavrini, L.R. Quitadamo, L. Bianchi, G. Saggio. "Combination of Classifiers using the Fuzzy Integral for Uncertainty Identification and Subject Specific Optimization - Application to Brain-Computer Interface". Proceedings of the International Conference on Fuzzy Computation Theory and Applications, 2014.

[10] G. McGimpsey, T.C. Bradford. "Limb Prosthetics Services and Devices, Critical Unmet Need: Market Analysis", Bioengineering Institute Center for Neuroprosthetics, Worcester Polytechnic Institution, 2015.

[11] D.K. Blough, S. Hubbard, L.V. McFarland, D.G. Smith, J.M. Gambel, G.E. Reiber. "Prosthetic cost projections for servicemembers with major limb loss from Vietnam and OIF/OEF". Journal of Rehabilitation Research & Development (JRRD), 2010.

[12] OttoBock's Michaelangelo Hand Brochure: "Fascinated with Michelangelo - Perfect use of precision technology". OttoBock HealthCare LP, 2014.

[13] B. Buntz, "An Advanced Prosthetic Hand that Costs $1000". Medical Product Manufacturing News, 2013.

[14] Myo Gesture Control Armband Official Website (accessed 18th of August 2017): https://www.myo.com/

[15] "MYOBOCK® Electrodes", Otto Bock HealthCare

[16] R.R. Seeley, T.D. Stephens, P. Tate. "Anatomy and Physiology" (8th edition). McGraw Hill, 2008.

[17] J.G. Webster. "Medical Instrumentation: Application and Design" (4th edition). John Wiley & Sons, Inc, 2010.

[18] A.L. Alphonso, B.T. Monson, M.J. Zeher, R.S. Armiger, S.R. Weeks, J.M. Burck, C. Moran, R. Da Voodie, G. Loeb, P.F. Pasquina, J.W. Tsao. "Use of a Virtual Integrated Environment in Prosthetic Limb Development and Phantom Limb Pain". Annual Review of Cybertherapy and Telemedicine, 2012.

[19] M. Ortiz-Catalan, N. Sander, M.B. Kristoffersen, B. Håkansson, R. Brånemark. "Treatment of phantom limb pain (PLP) based on augmented reality and gaming controlled by myoelectric pattern recognition: a case study of a chronic PLP patient". Frontiers in Neuroscience, 2014

[20] C. Dietrich, K. Walter-Walsh, S. Preißler, G.O. Hofmann, O.W. Wittec, W.H.R. Miltner, T. Weiss. "Sensory feedback prosthesis reduces phantom limb pain: Proof of a principle". Neuroscience Letters, 2012.

[21] J. Vogel, C. Castellini, P. van der Smagt. "MG-Based Teleoperation and Manipulation with the DLR LWR-III". IEEE/RSJ International Conference on Intelligent Robots and Systems, 2011.

[22] O. Fukuda, T. Tsuji, M. Kaneko, A. Otsuka. "A Human-Assisting Manipulator Teleoperated by EMG Signals and Arm Motions". IEEE Transactions on Robotics and Automation, 2013.

[23] K. Kiguchi, Y. Hayashi. "An EMG-Based Control for an Upper-Limb Power-Assist Exoskeleton Robot". IEEE Transactions on Systems, Man, and Cybernetics, 2012.

[24] M. Mulas, M. Folgheraiter, G. Gini. "An EMG-controlled Exoskeleton for Hand Rehabilitation". Proceedings of the 2005 IEEE 9th International Conference on Rehabilitation Robotics, 2005.

[25] V.E. Kosmidou, L.J. Hadjileontiadis. "Sign Language Recognition Using Intrinsic-Mode Sample Entropy on sEMG and Accelerometer Data". IEEE Transactions on Biomedical Engineering, 2009

[26] B. Hudgins, P. Parker, R.N. Scott. "A new strategy for multifunction myoelectric control". Biomedical Engineering, IEEE Transactions, 1993.

[27] F. Tenore, A. Ramos, A. Fahmy, S. Acharya, R. Etienne-Cummings, N.V. Thakor. "Towards the Control of Individual Fingers of a Prosthetic Hand Using Surface EMG Signals". Proceedings of the 29th Annual International Conference of the IEEE EMBS Cité Internationale, 2007.

[28] G.R. Naik, A. Al-Timemy, H.T. Nguyen. "Transradial Amputee Gesture Classification using an Optimal Number of sEMG Sensors: An Approach using ICA Clustering". IEEE Transactions on Neural Systems and Rehabilitation Engineering, 2015.

[29] C. Cipriani, C. Antfolk, M. Controzzi, G. Lundborg, B. Rosén, M.C. Carrozza, F. Sebelius. "Online Myoelectric Control of a Dexterous Hand Prosthesis by Transradial Amputees". IEEE Transactions on Neural Systems and Rehabilitation Engineering, 2011.

[30] R. Ahsan, M.I. Ibrahimy, O.O. Khalifa. "Electromyography (EMG) Signal based Hand Gesture Recognition using Artificial Neural Network (ANN)". 4th International Conference on Mechatronics (ICOM), 2011.

[31] F. Riillo, L.R. Quitadamo, F. Cravrini, E. Gruppioni, C.A. Pinto, N.C. Pastò, L. Sbernini, L. Albero, G. Saggio. "Optimization of EMG-based hand gesture recognition: Supervised vs. unsupervised data preprocessing on healthy subjects and transradial amputees". Biomedical Signal Processing and Control, 2014.

[32] X. Jiang, L.K. Merhi, Z.G. Xiao, C. Menon. "Exploration of Force Myography and surface Electromyography in hand gesture classification". Medical Engineering and Physics, 2017.

[33] P. Slade, A. Akhtar, M. Nguyen, T. Bretl. "Tact: Design and Performance of an Open-Source, Affordable, Myoelectric Prosthesis Hand". IEEE International Conference on Robotics and Automation (ICRA), 2015.

[34] K.F. Gretsch, H.D. Lather, K.V. Peddada, C.R. Deeken, L.B. Wall, C.A. Goldfarb. "Development of novel 3D-printed robotic prosthetic for transradial amputees" The International Society for Prosthetics and Orthotics, 2015.

[35] M. Polisiero, P. Bifulco, A. Liccardo, M. Cesarelli, M. Romano, G.D. Gargiulo, A.L. McEwan, M. D'Apuzzo. "Design and assessment of a low-cost, electromyographically controlled, prosthetic hand". Medical Devices: Evidence and Research, 2013.

[36] S. Masson, F.S. Fortuna, F.S. Moura, D.C. Soriano. "Integrating Myo Armband for the Control of Myoelectric Upper Limb Prosthesis". XXV Congresso Brasileiro de Engenharia Biomédica, 2016.

[37] D.S. Gonzales, C. Castellini. "A realistic implementation of ultrasound imaging as a human-machine interface for upper limb amputees". Frontiers in Neurorobotics, 2013.

[38] C. Nissler, N. Mouriki, C. Castellini. "Optical Myography: Detecting Finger Movements by Looking at the Forearm.". Frontiers in Neurorobotics, 2016.

[39] M.R. Dawson. "The Development of a Myoelectric Training Tool for Above-Elbow Amputees". 2011.

[40] R.H. Chowdhury, M.B.I. Reaz, M. A.B.M. Ali, A.A.A. Bakar, K. Chellappan, T.G. Chang. "Surface Electromyography Signal Processing and Classification Techniques". Sensors, 2013.

[41] E. Scheme, K. Englehart. "Electromyogram pattern recognition for control of powered upper-limb prostheses: State of the art and challenges for clinical use". Journal of Rehabilitation Research & Development, 2011.

[42] J.H. Holmes, P.L. Lanzi, W. Stolzmann, S.W. Wilson. "Learning classifier systems: New models, successful applications". Information Processing Letters, 2012.

[43] F. Lotte, M. Congedo, A. Lécuyer, F. Lamarche, B. Arnaldi. "A review of classification algorithms for EEG-based brain-computer interfaces". Journal of Neural Engineering, 2017.

[44] E. Alpaydin. "Introduction to Machine Learning" (2nd edition). The MIT Press, 2010.

[45] J. Platt. "Sequential Minimal Optmization: A Fast Algorithm for Training Support Vector Machines". Microsoft Research, 1998.

[46] G. Zararsiz, E. Coşgun. "Introduction to Statistical Methods for MicroRNA Analysis". Methods in Molecular Biology, 2014.

[47] F. Cavrini. "Hand gesture recognition for the benefit of transradial amputees". Master's thesis, Sapienza University of Rome, 2016.

[48] C. Sammut, G.I. Webb. "Encyclopedia of Machine Learning" Springer Science + Business Media, 2011.

[49] J. Wu, L. Sun, R. Jafari. "A Wearable System for Recognizing American Sign Language in Real-Time Using IMU and Surface EMG Sensors". IEEE Journal of Biomedical and Health Informatics, 2016.

[50] "13E200 Instructions for use", Otto Bock Healthcare Products GmbH

[51] D. Prutchi, M. Norris. "Design and Development of Medical Electronic Instrumentation: A Practical Perspective of the Design, Construction, and Test of Medical Devices". New Jersey: John Wiley & Sons, 2005

[52] MCP3304 by Microchip Datasheet (accessed 8th of November 2017): http://www.microchip.com/wwwproducts/en/MCP3304

[53] S. Benatti, F. Casamassima, B. Milosevic, E. Farella, P. Schonle, S. Fateh, T. Burger, Q. Huang, L. Benini. "A Versatile Embedded Platform for EMG Acquisition and Gesture Recognition". IEEE Trans. Biomed. Circuits Systems, 2015.

[54] Myo SDK Manual: https://developer.thalmic.com/docs/api_reference/platform/index.html

[55] Arduino's Official Website, where Arduino IDE can be downloaded for free (accessed 8th of November 2017): https://www.arduino.cc/en/main/software

[56] Official Website from Myo, where "Myo Data Capture" can be downloaded for free (accessed 8th of November 2017): https://market.myo.com/app/55009793e4b02e27fd3abe79/myo-data-capture

[57] Weka's Official Website (accessed 8th of November 2017): http://www.cs.waikato.ac.nz/ml/weka/

[58] R-Project Official Website (accessed 8th of November 2017): https://www.r-project.org/

[59] J. Demsar. "Statistical Comparisons of Classifiers over Multiple Data Sets". Journal of Machine Learning Research, 2006.